Clinical advances in cardiovascular magnetic resonace imaging and angiography

Bosch, H.C.M. van den

Chapter 4

Cardiovascular Magnetic Resonance Angiography: Carotids, Aorta, and Peripheral Vessels

Harrie CM van den Bosch
Jos JM Westenberg
Albert de Roos

based on
Chapter 45 Cardiovascular Magnetic Resonance Angiography: Carotids, Aorta, and Peripheral Vessels
in Cardiovascular Magnetic Resonance, 3rd Edition, 2018
Warren J Manning and Dudley J Pennell
Elsevier

Magnetic resonance angiography (MRA) is an important imaging modality for the diagnosis, clinical work-up and treatment planning in patients suspected for a wide range of vascular pathology. The aim of MRA is to visualize the arterial and/or venous system by creating high contrast between blood flow and its surrounding stationary tissue. To fulfill this aim, several techniques may be used in clinical practice. Depending on its demands and the conditions required to optimally visualize specific vessels of interest, imaging techniques are chosen. In the first part of this Chapter, techniques will be addressed that are currently available and applied for MRA. Contrast-enhanced MRA (CE-MRA) is probably the most widely used MRA technique. CE-MRA is applied either by fast imaging of the first-pass of an intravenously injected bolus of a gadolinium chelate agent, or by a prolonged imaging approach with a blood-pool contrast agent. The latter approach is applied when imaging requires a time window that surpasses the first arterial pass. Because of the reported adverse events (i.e., nephrogenic systemic fibrosis, accumulation of gadolinium in the brain, kidneys and bone tissue) associated with gadolinium (Gd)-based contrast agents, an increasing interest in non-CE-MRA techniques is currently observed. Black-blood and bright-blood non-CE-MRA techniques will be discussed. Finally, flow imaging by time-resolved three-dimensional phase contrast (i.e. 4D flow MRI), with the aid of newly developed visualization tools, is a relatively new technique that may be used to visualize complex flow structures and add quantitative hemodynamic information as well.
In the second part of this Chapter, we will address the anatomical regions that are imaged by MRA and discuss the state-of-the-art. Special focus will be on the carotid arteries, thoracic and abdominal aorta, renal arteries, mesenteric artery, and the peripheral arteries.

Contrast Enhanced MR Angiography: technical approach

In CE-MRA, vessels in the field-of view of interest are imaged during the arterial first-pass of intravenously injected paramagnetic contrast material.[1] These contrast agents have a short T1 relaxation time and will produce high signal on T1-weighted images. In clinical practice, Gd-bound chelates, for example DTPA (diethylenetriamine pentaacetic acid), are used as paramagnetic contrast agents. The gadolinium ion is a rare-earth element, and toxic to humans when unbound. Therefore, in MRI, gadolinium contrast is based on chelates and thereby, controlling the distribution of gadolinium within the body and to overcome toxicity however maintaining their contrast enhancement capacity. A very important property of these chelates is their chemical stability, which depends on the chemical structure and ionicity of the complex.[2] A stable chelate has less tendency to release free gadolinium ions in the

human body. Gadolinium chelates can be distinguished in two structural categories: macrocyclic and linear gadolinium chelates. In macrocyclic structures, the gadolinium chelate is more stable and, therefore, the chance of free gadolinium ions in the body is reduced. Breaking of the bond between gadolinium and the chelate (transmetallation) is more likely to occur with linear agents than with macrocyclic agents. However, even the fact that macrocyclic agents are more resistant to transmetallation, development of NSF is described in patients with severe renal failure after several gadolinium contrast administrations.[3] Most reported cases of nephrogenic systemic fibrosis are linked with linear Gd-chelates. Awareness of this association has given rise to effective screening of patient with possible renal failure, use of more stable Gd-chelates, and international recommendations for the use of Gd-based contrast agents in daily practice.[4,5,6]

Gd-chelates create intravascular signal by shortening the T1 relaxation time of blood in proportion to the concentration of contrast material. At 1.5T, T1 of blood is 1200 ms. The T1 relaxation time is shortened by gadolinium according to equation 1[7]:

$1/T1 = 1/1200\ ms + R_1[Gd]$ *{Equation 1}*

R_1 = T1 relaxivity of gadolinium, [Gd] = gadolinium concentration in blood.

Gadolinium-enhanced MRA is insensitive to blood flow, in contrast to non-CE-MRA techniques as time-of-flight (TOF) and phase-contrast (PCA) MRA. Consequently, in CE-MRA, image quality is not degraded by flow disturbances.

Gadolinium contrast agents can be classified depending on their distribution in tissue after intravenous administration, e.g. extracellular or intravascular. Most of the gadolinium chelates used in clinical routine are extracellular agents. After intravascular administration they diffuse rapidly through the capillary walls into the extravascular space. In CE-MRA, arteries are preferably imaged during the initial passage of contrast. Timing of starting the image acquisition is essential to reduce signal from gadolinium diffused to the extracellular space and to overcome venous enhancement, which can lead to artifacts and image degradation.

The application of CE-MRA was improved by the introduction of Gd-chelates that have the capability to bind to larger molecules in the blood such as albumin. These contrast agents (e.g. gadobenate dimeglumine) provide a prolonged imaging time window due to a decreased decay time of contrast in blood. The use of such agents enables imaging beyond the initial passage of contrast bolus, which may be a benefit when acquisition needs to be gated to cardiac or respiratory motion, or when high resolution is required in small vessels such as the coronaries.[8] When compared to an extravascular Gd-chelate, blood pool agents show an improved conspicuity of small vessels (9). Further development of macromolecular blood pool agents in the near future may play an important role in CE-MRA.

3D Contrast-enhanced MRA Pulse sequences

The MRI sequence that is used in CE-MRA needs to fulfill the following needs: T1-weighting is required as well as obtaining a large 3D volume with sufficient spatial resolution, preferably fast within the first-pass of contrast and within a breath hold to suppress respiratory motion. Therefore, fast T1-weighted 3D spoiled gradient-echo (GRE) sequences are used for image acquisition. In clinical routine, 3D CE-MRA preferentially is performed on a 1.5T or 3T system with strong gradient systems to reduce scan time as such that 3D datasets can be acquired during breath-holding. Typically, short repetition times (TR) and echo times (TE) are used, 3-8 ms and 1-3 ms, respectively. Flip angle is 20^{o}-40^{o} to achieve optimized T1-weighting.
Furthermore, subsampling imaging techniques such as parallel imaging are implemented to reduce total scan time.[10] Advanced k-space sampling techniques (spiral, keyhole, echo planar imaging) may be used as well to speed up acquisition.
At postprocessing, the 3D nature of the dataset allows viewing of the data from any desired angle, i.e. by creating multi-planar reformats (MPR) or rotational maximum-intensity-projection (MIP). This results in multiple images in various anatomic orientations. Thin (i.e., <3 mm thick) slices are required in order to provide a useful evaluation of these images. In some situations, it may be useful to use thicker slices (e.g., 10 mm) to reduce the number of slices and allow faster scanning. Although the ability to rotate the MIP is lost with such thick slices, scan times can be as short as 1 second.

Bolus timing

Precise bolus timing is essential for first-pass CE-MRA. Arterial imaging is performed in the time window between arterial and venous enhancement and this time window depends on the rate of contrast agent injection, and will be patient specific.[11] The transit time of contrast from the injection site (usually in the veins in the arm) to the field-of-view with the vessels of interest depends on several factors, e.g. injection rate, injection site, heart rate, and stroke volume.
The gadolinium contrast concentration in the arterial blood is proportional to the injection rate and inversely proportional to the cardiac output:

$[Gd]_{arterial}$ = injection rate (mol/sec) / cardiac output (L/sec) *{Equation 2}*

T1 for blood is related to the injection rate and cardiac output by combining equation 1 and 2.[12]
Maximum arterial signal intensity is achieved when the start of the acquisition and the contrast infusion are synchronized such that peak arterial gadolinium concentration coincides with the acquisition of the central portion of k-space.[13] The center of k-space contributes most to overall image contrast, whereas the periphery of k-space

provides image information of details and contributes to spatial resolution. Therefore, for improved arterial/venous differentiation central k-lines have to be sampled before venous return. In CE-MRA, different types of k-space filling can be used in the available 3D pulse sequences. It is important to adjust bolus timing to the order of k-space filling used.
In linear ordering, lines of k-space can be acquired in any order (high k-space lines first, low k-space lines first, or at random). Linear ordering can be used in a CE-MRA protocol when precise timing of the contrast bolus is difficult or arrival time may be prolonged.
For most CE-MRA examinations, elliptical-centric ordering is the preferred k-space sampling method used. Typically, the center of k-space is acquired first and the periphery later (e.g. elliptic-centric, CENTRA ("Contrast-ENhanced Timing Robust Angiography"),[14] DRKS ("Differential Rate K-space Sampling"), or PEAKS ("PEak Arterial K-Space filling")).
To determine the delay between the start of the venous contrast injection and the start of the acquisition, either a small test bolus or fluoroscopic real-time imaging can be used. The timing method by using a test bolus (1 to 2 mL) is robust and easy to perform. However, it will lengthen the procedure with a few minutes and requires an additional administration of contrast. In fluoroscopic real-time imaging, the inflow of contrast is imaged in the field-of-view with the vessels of interest. At the moment of contrast arrival, the acquisition is started automatically, however, a disadvantage can be the short delay of a few seconds, which is needed to switch from the fluoroscopic real-time imaging to the actual start of CE-MRA acquisition.

Contrast-enhanced versus non-contrast-enhanced MRA

In recent years the association between CE-MRA and nephrogenic systemic fibrosis (NSF) has been reported.[15,16] The occurrence of NSF has been described exclusively in patients with severe renal failure and developed most frequently after administration of linear Gd-chelates.[4]
Moreover, gadolinium accumulation in tissue in patients without renal impairment has been reported in several studies. Kanda et al. reported residual gadolinium concentrations in the brain, particularly in the dentate nucleus and globus pallidus, of patients without severe renal dysfunction[17] and foci of hyperintensity on unenhanced T1-weighted MR images associated with previous administration of linear Gd-chelates and may be associated to the total number of previous gadolinium-based contrast material administrations.[18] Deposition of gadolinium has also been demonstrated in bone, skin, and, liver.[19,20]

Currently, previous administration of macrocyclic Gd-chelates showed no association with gadolinium accumulation in tissue yet,[21,22] however, these macrocyclic contrast chelates have been in use in clinical practice for a shorter time than the linear chelates.
Nevertheless, the application of CE-MRA and the amount of administered contrast is of clinical importance, especially in patients with impaired renal function. Awareness of NSF-related incidents associated with CE-MRA and reports on accumulation of gadolinium in various tissues have also led to a renewed interest in non-CE-MRA. Improvements in MR hardware and software, including the widespread availability of parallel imaging have helped to reduce acquisition times and have made some non-CE-MRA methods clinically practical.
Non-CE-MRA methods may be classified into three categories, black-blood, bright-blood and 4D flow visualization.

Black-blood imaging

Black-blood imaging of blood vessels uses double-inversion recovery to null the signal of flowing blood.[23] This technique is flow-sensitive. Two 180º inversion recovery prepulses are applied to null the signal of flowing blood: the first prepulse is non-slice selective and inverts the longitudinal magnetization vector in the entire body, while the second prepulse is slice selective and inverts the magnetization in the imaging slice back to its original orientation. Signal of blood entering the imaging slice after the second prepulse has undergone reinversion and will appear dark in the images. ECG-gated partial Fourier Fast Spin-Echo (FSE) is the sequence of choice,[24,25] using a slice thickness of 6 to 8 mm stacked in the transverse plane of the chest or in a double-oblique sagittal view of the aorta (i.e., the candy cane view). Single-shot FSE (SSFSE) sequences are much faster than basic FSE sequences and allow for acquisition of the entire imaging stack in a single breath-hold. Fat saturation is recommended to increase the conspicuity of aortic wall hematoma.[26] Despite being an established technique, black-blood imaging is prone to artifacts, as inadequate nulling of blood signal may occur by slow flow, or when in-plane blood flow is present.

Bright-blood imaging: Time-Of-Flight (TOF)

TOF methods depend on the inflow enhancement of flowing blood and the relative saturation of longitudinal magnetization of stationary tissue to produce high contrast. The longitudinal magnetization from the background tissue is suppressed by multiple RF excitations, such that the magnetic spins associated with background tissue do not have sufficient time to fully regain their longitudinal magnetization. Saturation of background signal will reach a steady-state determined by the flip angle, repetition

time and the T1 of the background tissue. This saturation will make stationary tissue appear dark in TOF images. The bright signal intensity of flowing blood is the consequence of the continuous inflow of fresh, unsaturated blood into the imaging slice, which produces more signal than the surrounding stationary tissue, as the latter was repeatedly exposed to RF pulses.[27] This effect is known as flow-related enhancement[28] and can be maximized by using sequences with a short repetition time (TR). Ideally, the imaging slice should be thin and oriented perpendicular to the direction of flow. Electrocardiographic (ECG) gating can be used to optimize synchronization of acquisition to the blood flow to the cardiac cycle and consequently to the signal present in the artery of interest.
2D and 3D TOF techniques are in use. 2D TOF with consecutive slices stacked together can produce excellent contrast in the vessels when the imaging slices are planned perpendicular to the vessels of interest. When in-plane flow occurs, the longitudinal magnetization of blood will become saturated and signal is progressively lost. Additionally, venous signal may be suppressed with presaturation slabs, positioned parallel and next to the imaging slices, in order to saturate longitudinal magnetization of blood flowing into the imaging slice from the opposite side of arterial blood flow. Resolution of 2D TOF is often limited by the used slice thickness. However, thin slice acquisitions are possible, but acquisition time will increase with the amount of slices required to cover the vasculature and signal-to-noise ratio will decrease with decreasing slice thickness.
3D TOF may be performed with isotropic voxel sizes of 1 mm^3. High resolution is essential to visualize small branch vessels, stenosis or to provide a clear delineation of tortuous vessels. 3D TOF has to deal with saturation effects of arterial blood flow, especially slow flow. On the other hand, SNR will be increased by using 3D imaging. Decreasing the flip angle may reduce excessive saturation effects.

Bright-blood imaging: Phase Contrast Angiography (PCA)

In PCA, the contrast between flowing blood and the surrounding stationary tissue is generated by the flow-induced phase shift in the transverse magnetization of the moving blood. As the magnetic field strength and the precession frequency of spins are linearly related, the precession frequency will increase when spins move along a positive gradient in the magnetic field. Compared to spins that remain fixed in position (i.e., in stationary tissue), moving spins (i.e., in flowing blood) will accumulate phase in the transverse magnetization. This phase shift is proportional to its velocity and the gradient strength.[29] In addition to such a velocity-sensitive acquisition, a velocity-compensation acquisition is defined. Such acquisition uses a bipolar gradient with equal positive and negative effect to achieve no difference in net phase shift between spins moving with uniform velocity. PCA uses the subtraction of both velocity-sensitive and velocity-compensation acquisitions to visualize moving spins.

The velocity can be directly quantified from the resultant phase images. A priori to the acquisition the velocity sensitivity needs to be determined by choosing the Venc, i.e., the outer limit of the velocity range that is encoded by the phase shift of +180° and -180°.

TOF and PCA, two conventional bright-blood non-CE-MRA techniques, were highly time consuming and moreover, suffered from artifacts caused by turbulence and in-plane saturation. In a meta-analysis,[30] the sensitivity and specificity for the detection of significant stenosis (>50% luminal reduction) for 2D TOF ranged from 64% to 100% and 68% to 96%, compared to 92% to 100% and 91% to 99%, respectively for CE-MRA. Such limitations resulted in declining interest for TOF and PCA in favor of CE-MRA. However, in association with the reported adverse events from gadolinium usage, an increase in interest in new bright-blood non-CE-MRA techniques is occurring.

Bright-blood imaging: Steady-State Free-Precession (SSFP)

SSFP produces high signal intensity for blood, due to the inherently T2/T1-weighted image contrast which is high for all fluids, independent from inflow effects. ECG-gated cine acquisitions with SSFP are used to visualize the anatomy of thoracic aorta with breath-hold sequences. Aneurysms, coarctation and stenosis or dissection flaps can be visualized using this approach. The aortic root is best evaluated in multiple planes, including long-axis planes of the left ventricular outflow tract (LVOT). The remainder of the thoracic aorta is best evaluated with images in the transverse plane of the chest and in the double-oblique sagittal candy-cane view. SSFP sequences are susceptible to magnetic field inhomogeneity, which are particularly present at high field strength. Off-resonance artifacts may result in non-diagnostic images. Dedicated shimming algorithms may aid in minimizing these off-resonance artifacts.

Bright-blood imaging: Dixon

Another relatively new bright-blood approach relies on an old technique based on the chemical shift between both water and fat. Dixon's water-fat separation[31] uses the phase shift from the water-fat resonance frequency and by using carefully chosen multiple echo times, excellent separation between water and fat is achieved in four distinct images: separate water and fat images as well as images with signal from both tissues in- and out-of-phase. The Dixon technique may be applied for MRA purposes, its application may be promising for imaging of the coronaries as well as the thoracic aorta.[32]

Blood flow visualization with 4D flow MRI

Phase-contrast imaging enables quantitation of blood flow velocity in the direction of a magnetic field gradient. In addition to conventional through-plane one-directional velocity-encoding, advanced 3D time-resolved imaging is possible with velocity-encoding in all three directions, providing the temporal distribution of a velocity vector field, representing the flow of blood inside a 3D volume (i.e., so-called 4D flow data).[33] Visualization tools such as streamline and pathline visualization have been developed to display this data and to segment blood vessels of interest from their surrounding tissue. The usability of this technique has been shown in the aorta and pulmonary arteries, the carotid artery, the abdominal circulation as well as the circulation in the brain. While this technique is still a research application, a lot of effort has been made in recent years to translate this technique towards the clinic.[34] The additional hemodynamic information (e.g. wall shear stress, stenotic pressure drop, pulse wave velocity, viscous energy dissipation) which becomes available with 4D flow MRI in combination with the excellent 3D visualization possibilities of complex vascular structures and pathologies, may eventually push this modality towards a clinical viable application.

Artifacts in CE-MRA

In CE-MRA, images with maximum arterial signal intensity are obtained when the acquisition of the central portion of k-space coincides with peak arterial gadolinium concentration. Timing of bolus arrival and imaging within the time window of arterial enhancement is critical to minimize artifacts. Starting the acquisition too early, when the contrast bolus is still arriving in the vessels of interest, can cause ringing or so-called Maki artifacts.[13] Starting the acquisition too late will lead to imaging outside the time window of arterial enhancement, causing venous enhancement hampering the evaluation of arterial vasculature. Such artifacts may result in degradation of image quality and misclassified diagnosis.

Artifacts are most evident when the center of k-space is acquired before the peak of intravascular gadolinium arrival.[13] The Maki artifact for example, results in a central dark line in the vessel, from which a so-called pseudo-dissection can appear, when the contrast bolus arrives in the vessel of interest after sampling of the central k-lines. Overestimation of the length of a stenosis can occur due to signal loss because of turbulence and in-plane saturation. Generally, this latter artifact is not present in CE-MRA, however, signal loss can occur in the stenosis caused by high velocity rates, especially in combination with low contrast material concentration.[35]

Erroneously, an occlusion can be apparent in tortuous arteries when the vessel of interest is not completely covered inside the field-of-view. Parallel to vessels with very high signal intensity ghosts (i.e. phase artifact) can be seen.[36]
Movement of the patient between the acquisition of the mask and the CE-MRA may lead to subtraction artifacts, leading to image degradation. Signal loss caused by susceptibility can be seen when clips, metallic stents or prostheses are present.

In non-CE-MRA, artefacts may also results in image degradation or even lead to misdiagnosis. Post-stenotic signal loss due to turbulence or in-plane saturation in phase contrast imaging may lead to an overestimation of a stenosis. When the a priori set velocity sensitivity (Venc) is too low, aliasing will occur in the velocity images and when uncorrected will result in a decrease in signal in the phase contrast magnitude images.
On the other hand, slow flow in TOF imaging may lead to similar misdiagnosis when vascular signal decreases. In black-blood imaging, in-plane flow may lead to vascular enhancement and inadequate signal suppression when the imaging slice is too thick.
SSFP is very susceptible to off-resonance artifacts, especially at higher field strength and non-optimal shimming, which may degrade image quality to the point of non-evaluable for clinical diagnosis.

Magnetic resonance angiography of the extracranial carotid arteries

Atherosclerosis of the extracranial carotid arteries is an important cause of stroke.[37] Worldwide stroke is a major health concern, for example approximately 795,000 patients with a stroke are reported in the United States every year.[38] Around 610,000 patients are new attacks and 185,000 patients experience a recurrent episode of stroke. Stroke can lead to significant disability in nonfatal cases and accounts for approximately 1 of every 20 deaths in the United States.
Carotid atherosclerosis is a significant factor for risk stratification and is associated with more than a doubling in the risk of stroke after a transient ischemic attack.[39]
Therefore, accurate evaluation of the extracranial carotid artery is essential.
For evaluating the severity of carotid stenosis, digital subtraction angiography (DSA) remains the standard of reference. This imaging approach has certain limitations, including invasiveness and the use of ionizing radiation. Moreover, DSA involves a small risk of stroke on the order of around 0.5-4%.[40]
Therefore, nowadays non-invasive imaging techniques play an important role in the routine assessment of patients with suspected carotid artery. Non-invasive techniques

as duplex ultrasound (DUS), CE-MRA and computed tomography angiography (CTA) are widely available and have replaced invasive arteriography in daily clinical routine.
When compared to DSA, non-invasive imaging techniques generally are less accurate for low degree carotid artery stenoses. Meta-analysis showed sensitivity and specificity for DUS of 36% and 91% respectively for 50% to 69% stenosis degree of the internal carotid artery, 77% and 97% respectively for CE-MRA, and 67% and 79% respectively for CTA.[41] Non-invasive techniques revealed higher sensitivity and specificity for high grade stenosis (70%-99%), DUS 89% and 84%, CE-MRA 94% and 93%, and CTA 77% and 95%, respectively.
Duplex ultrasound is widely available, easy accessible, cost-effective and often used as a first line investigation in standardized protocols assessing carotid vascular disease.[42] In experienced hands it is an accurate test, however it has higher interobserver variability and lower sensitivity and specificity when compared to CE-MRA and CTA. Guidelines of the American Heart Association (AHA) and the American College of Cardiology Foundation recommend evaluation of the carotid artery by MRA or CTA, when DUS provides equivocal or non-diagnostic results.[43] When DUS detects a significant stenosis (>70%) it is useful to evaluate stenosis severity by performing MRA or CTA. For assessing carotid artery stenosis, CE-MRA show a comparable accuracy.
However, CTA has some limitations. CTA requires the use of ionizing radiation and administration of larger intravenous contrast volumes, application iodinated contrast with possible toxicity and adverse reaction, and, moreover, calcification in plaque may hamper stenosis gradation. Therefore, it is becoming common practice to combine DUS, as first line screening modality followed by CE-MRA for gradation of carotid stenosis.
CE-MRA is the MRA technique of choice to evaluate carotid vascular disease (Figure 4.1). Typically, 3D CE-MRA data are acquired in a coronal plane. In CE-MRA of the carotid arteries bolus timing is essential, since venous return in the neck veins occurs fast. Spatial resolution of 0.71 mm^3 at 1.5T and 0.54 mm^3 at 3T are recommended.[44] Generally, single dose of gadolinium-based contrast agent (0.1 mmol/kg) is sufficient to achieve excellent image quality and resolution at 1.5T. Several studies showed that dose reduction to half dose (0.05 mmol/kg) is feasible at 3T without compromising SNR and spatial resolution.[45,46]
In several studies TOF MRA showed good sensitivity and specificity in detecting stenosis of the carotid bifurcation.[47,48] However, CE-MRA offers high resolution imaging of larger field-of-view in shorter acquisition times[49,50] and therefore, has replaced TOF MRA in clinical practice.
Development of new non-CE-MRA sequences show promising results and could have the potential to become an alternative imaging approach in evaluating carotid vascular disease. Zhoa et al.[51] showed that 3D black-blood MR imaging provided high agreement for stenosis measurements as compared to DSA. 3D black-blood MR imaging depicted longer lesion length than DSA, because it is able to define vessel wall

morphology and distribution of plaque. When compared to CE-MRA, 3D black-blood MRA show accurate measurement of carotid stenosis[52] and sensitivity and specificity comparable with CTA.[51]

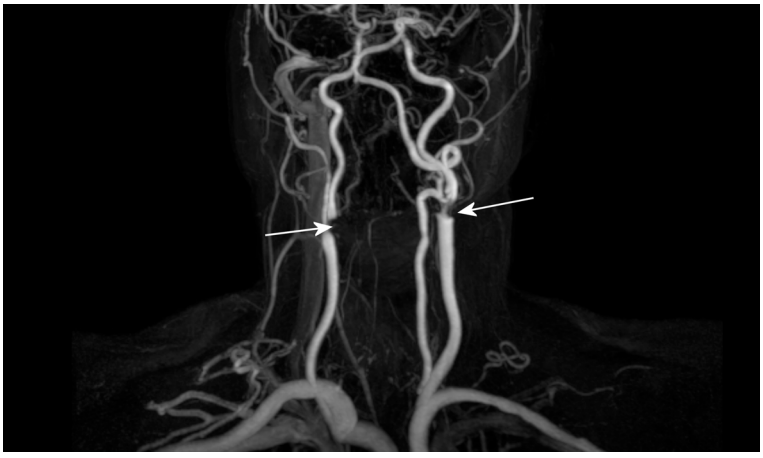

Figure 4.1 CE-MRA shows a significant stenosis of the proximal internal carotid artery on both sides (arrows).

Other vascular disease of the carotid artery can also be diagnosed by CE-MRA. Fibromuscular dysplasia (FMD) is a non-atherosclerotic, non-inflammatory arteriopathy with segmental involvement of small- and medium sized arteries. The etiology is unknown and the extracranial carotid, vertebral, and renal arteries are most frequently affected. The so-called string-of-beads sign of the involved arteries is a classic pattern seen in FMD, but also other imaging findings are described, as aneurysm, fusiform arterial ectasia, and vascular loops. FMD can accurately be diagnosed using CE-MRA, however, a negative result on CE-MRA does not rule out the diagnosis of FMD. Therefore, DSA is still mandatory in patients with high clinical suspicion of FMD.[53]

Carotid artery dissection is one of the most common causes of stroke in young patients. Dissection can occur after trauma, but may arise spontaneously. In patients suspected for carotid artery dissection, CE- MRA is the imaging modality of choice.[54,55] Mural hematoma can be visualized by performing additional axial T1W images with fat suppression. Although DSA is the reference standard for evaluation of the lumen of the carotid artery, it does not provide details of the arterial wall. In suspected cases it is important to reformat acquired high-resolution isovolumetric voxels in axial thin slices to eventually depict an intimal flap.

Magnetic resonance angiography of the aorta

Diseases of the thoracic and abdominal aorta can be examined by several imaging modalities. Over the last decade non-invasive imaging techniques have improved significantly and therefore, the need for DSA as imaging tool in clinical practice has decreased. With non-invasive techniques the risks of arterial catheterization and the use of iodinated contrast medium can be avoided.

A wide spectrum of vascular diseases affecting the thoracic and abdominal aorta can be evaluated by angiographic imaging, including aortic aneurysm, suspected aortic dissection, penetrating atherosclerotic ulcer, arterial occlusive disease in atherosclerosis, genetic diseases (e.g. Marfan syndrome), and congenital abnormalities such as coarctation of the aorta. For imaging the thoracic aortic lumen, current established non-invasive techniques such as transthoracic echocardiography (TTE), transesophageal echocardiography (TEE), MRA and CTA are able to provide additional information of the aortic wall and the relationship of vascular disease to surrounding tissue. Echocardiography is most commonly used as a first line imaging modality, but also MRA and CTA are widely used. The abdominal aorta is most typically imaged by ultrasound, MRA, and CTA,[56] whereas echocardiography is the most frequently used imaging modality for evaluating the aortic root and proximal ascending aorta.

In a standardized echocardiographic examination the thoracic aorta is routinely assessed.[57] Despite the fact that TTE is limited for assessing the complete thoracic aorta, it still permits adequate assessment of several aortic segments, especially adequate when monitoring aortic root diameters.[58] Moreover, TTE can be used as a screening tool for proximal ascending aorta dilatation.

Due to the proximity of the esophagus to the thoracic aorta, TEE is often used in thoracic aorta assessment to overcome the limitations of TTE. TEE reveals high resolution images and unlike TTE allows gradual assessment of the thoracic aorta from the aortic root to the descending aorta.[59,60] However, if echocardiography reveals inconclusive information or when abnormalities are present, another imaging modality is required for further work-up.

CTA is an important imaging technique in vascular diseases of the thoracic and abdominal aorta. Especially in acute aortic syndrome (i.e. aorta dissection, intramural hematoma, penetrating atherosclerotic ulcer, and contained aortic rupture) CTA plays a key role and is the preferred primary imaging technique. Multi-slice CT scanners are widely available and can provide images with high spatial resolution. Therefore, CTA has essentially replaced invasive DSA. Diagnostic accuracy of CTA for the detection of dissection and traumatic injury are excellent. Sensitivity and specificity for the detection of dissection are 100%.[61] Steenburg et al.[62] reported a sensitivity of 96.0%, a specificity of 99.8%, and accuracy of 99.8% for multislice CTA as compared with DSA in patients with acute thoracic aortic injury.

The role of MRA in the evaluation of acute aortic syndrome is limited. Monitoring acute, unstable patients in the MRI scanner is more complicated and acquisition times are longer. However, MRA has several advantages over CTA such as the above mentioned radiation-free nature of the imaging modality in which the need for iodinated contrast medium is avoided. Therefore, MRA is highly suitable for evaluation of aortic disease in young patients and for follow-up studies.[63]
CE-MRA has emerged as the preferred MRA technique for evaluation of thoracic and abdominal vascular pathology independent of blood flow. High-resolution 3D image acquisition permits multi-planar and MIP reconstructions in any desired plane for detailed image evaluation (Figure 4.2). 3D CE-MRA acquisition does not require ECG triggering and can be performed during a single breath hold of approximately 15 to 20 seconds.

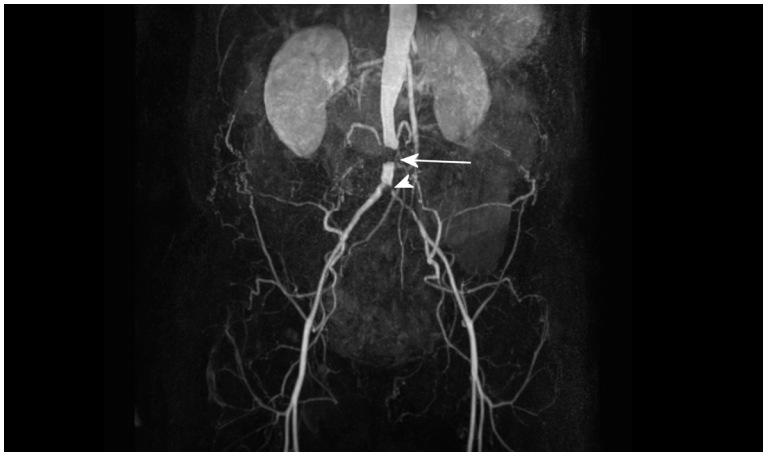

Figure 4.2 CE-MRA shows a short distal aortic occlusion (arrow) and a significant stenosis of the proximal left common iliac artery (arrowhead).

For optimizing SNR surface phased-array coils are used for imaging the thoracic and abdominal aorta, however, sufficient image quality can also be achieved by applying the body coil. Positioning of the surface phased array coil in thoracic aorta imaging is important as the volume stack should include the proximal brachiocephalic arteries. When imaging the abdominal aorta, positioning of the 3D volume is essential such that the acquired volume contains the proximal course of major arterial braches as the cephalic trunk, superior mesenteric artery, renal arteries and iliac arteries.
For both the thoracic and abdominal aortic CE-MRA, patients are routinely imaged in supine position.

The imaging protocol of the thoracic aorta consists of a survey or localizer sequence, SSFP cine imaging, contrast bolus timing sequence (test bolus or fluoroscopic real-time imaging), 3D CE-MRA sequence pre- and post-contrast and, depending on vascular disease, T1-weighted post-contrast sequence to rule out for example aortitis. Single-shot fast spin echo or SSFP acquired during breath holding can serve as a localizer sequence in three directions. For optimal planning and positioning of the 3D CE-MRA imaging volume, it is essential that the survey scan is performed in the same breath holding position as utilized for the 3D CE-MRA acquisition. Preferably, this breath holding is end-expiration since end-expiration is more reproducible when compared to end-inspiration.[64] SSFP images are acquired with ECG triggering and during breath holding. Preferably, two directions (axial and parasagittal planes) are acquired. SSFP images provide additional information about the vessel wall and surrounding tissue.

The pre-contrast 3D scan is acquired to verify proper positioning of the 3D volume and to rule out possible aliasing artifacts. For 3D CE-MRA, 0.1–0.2 mmol/kg body weight contrast medium is administered. The 3D dataset can be obtained in coronal, sagittal, or parasagittal plane. Covering the thoracic aorta in a coronal plane requires a larger volume and consequently, longer breath holding maintaining high spatial resolution. Therefore, in clinical practice, sagittal or parasagittal plane is favored. Typically, the field-of-view ranges from 30 to 40 cm.

Usually, the abdominal aorta is imaged in the coronal plane and the field-of-view varies between 35 and 40 cm. For both thoracic and abdominal CE-MRA, spatial resolution of at least 1–1.5 mm should be used.[65]

In CE-MRA of the thoracic and abdominal aorta, optimally two post-contrast datasets are obtained. Large aneurysms or false lumen in aortic dissection may have slow flow and therefore, require a longer time interval between contrast injection and 3D image acquisition to become fully enhanced. As a consequence, they may be only fully established during the second 3D volume acquisition. Moreover, distinction between slow flow and therefore potential non-filling with contrast of the lumen can be distinguished better from thrombus.

Additionally, ECG-triggered T1-weighted images with fat suppression can be acquired to analyze the aortic wall. Phase contrast sequences can be performed to quantify flow.

Non-CE-MRA of the thoracic aorta can also provide additional information of the aortic wall and surrounding tissue, and therefore, this acquisition is an important sequence within the standard MRA imaging protocol. Non-CE-MRA by SSFP may serve as a useful alternative for evaluation and follow-up of aortic disease when compared to CE-MRA in patients with contraindications to gadolinium use or with poor intravenous access. SSFP showed high diagnostic accuracy for aortic dimensions and vascular pathology, and similar reader confidence, when compared to CE-MRA.[66,67]

For the detection of aortic disease, free breathing 3D SSFP MRA with navigator gating

showed a 100% diagnostic accuracy with CE-MRA serving as reference standard.[68] Furthermore, SSFP showed significantly higher image quality of the aortic root, whereas non-ECG-gated CE-MRA images may suffer motion artifacts in this region hindering diagnostic image evaluation.

In CE-MRA, post-processing of the acquired 3D dataset is essential. On MPR and MIP reconstructions aortic vascular pathology can be assessed in relation to the origin of branching vessels. For serial follow-up examinations in patients with aortic dilatation, consistency and accuracy of aortic diameter measurements is critical, since increase in diameter may have important impact on risk stratification and on planning of surgical intervention.[69,70] The maximal diameter should be measured perpendicular to the axis of flow, double oblique or so-called centerline reconstruction.[71] Double oblique measurements of aortic diameter provided better agreement with the reference standard of planimetry than axial measurements and therefore, may have potentially important impact on surgical decision-making.[72]

Aneurysm of the thoracic aorta is often an incidental finding during TTE for cardiac screening or on chest X-ray in asymptomatic patients. Aortic aneurysm may lead to aortic rupture or aortic dissection. These acute events may be rapidly fatal in a large proportion of patients,[73] therefore, serial follow-up examinations in this patient population is vital. CE-MRA is a robust and accurate imaging modality for evaluation of the entire aorta and is favorable for long-term follow-up examinations without the need of ionizing radiation or iodinated contrast (Figure 4.3).

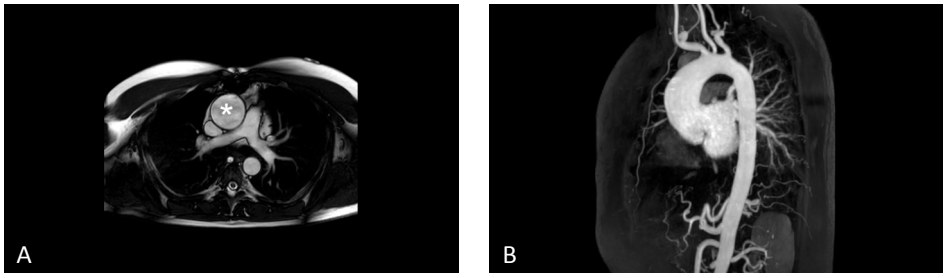

Figure 4.3 **(A)** Bright-blood steady-state free-precession axial image shows an aneurysm of the ascending aorta (asterix). **(B)** 3D CE-MRA (sagittal maximum-intensity-projection) of the same patient.

Reports showed a high accuracy for the detection of thoracic and abdominal aneurysms with a sensitivity of 100% and specificity of 100%, respectively, when compared to surgery or DSA.[74,75]

Atherosclerosis more often causes aneurysm formation in the descending and abdominal aorta, whereas dilatation of the ascending aorta more frequently occurs in aortic valvular disease as in aortic valvular regurgitation and in patients with bicuspid

valves. Other causes of aortic aneurysm are connective tissue disease (i.e. Marfan syndrome, Ehlers-Danlos, and Loeys-Dietz syndrome), Turner syndrome, inflammatory disease, trauma, chronic dissection or aortic surgery. Hypertension, smoking, hypercholesterolemia, and low high-density lipoprotein cholesterol are also significantly associated with aortic dilatation.[76,77]

Aneurysms can be classified in true and false aneurysms. A true aneurysm involves all three layers of the aortic wall, i.e. the intima, media, and adventitia. In a so-called false aneurysm, a disruption in the arterial wall causes blood leakage and an aneurysm contained by only the adventitia or surrounding tissue. The disruption may be caused by trauma, iatrogenic origin (e.g. percutaneous or surgical procedures), or inflammation. Risk of aneurysm rupture is higher in a false aneurysm when compared to true aneurysms.[78]

Morphologically, two types of aneurysms can be recognized: fusiform and saccular aneurysms. A fusiform aneurysm is concentric and involves dilatation of the full circumference of the aortic wall. A saccular aneurysm is eccentric and consists of a asymmetric outpouching of a part of the artic wall.

Bacterial infections of the aortic wall can cause the formation of mycotic aneurysms. The most common infecting organisms are Staphylococcus aureus and Salmonella. Mycotic aneurysms are usually saccular and are more prone to rupture. For optimal treatment early diagnosis is essential. Normally, patients present with signs of infection, including fever or sometimes sepsis. Often bacteremia is present, however negative blood cultures do not rule out the presence of mycotic aneurysm.[79] Therefore, imaging is very important for diagnosis. Besides the saccular aneurysm, CE-MRA can demonstrate additional perivascular inflammatory changes as soft tissue inflammation, edema, gas, and irregularity of the aortic wall leading to the diagnosis of mycotic aneurysm.

In aortic dissection, intraluminal blood penetrates into the media layer of the aortic wall through a tear in the intima, thereby dissecting the aortic wall. The proximal ascending aorta and the descending aorta distal to the origin of the left subclavian artery are the two most common sites where the aortic dissection is initiated and the intimal tear occurs. The bleeding between the dissected layers of the aortic wall forms the false lumen. Distention of the false lumen may narrow and compress the true lumen. Bleeding within the medial layer of the aortic wall can also cause the formation of a localized intramural hematoma (IMH) and facilitate the development of an intimal tear.

Currently, two classification systems - DeBakey and Stanford classification - are most frequently used for aortic dissection.[80] The DeBakey classification subdivides aortic dissection in type I, II, and III. In DeBakey type I aortic dissection the ascending and descending aorta are involved, in type II only the ascending aorta and aortic arch, and in type III the ascending aorta and arch are spared. The Stanford classification differentiates type A and type B aortic dissection. Type A involves the ascending aorta,

and eventually extending distally. Type B aortic dissections start out in the descending aorta and spare the ascending aorta and arch. If not operated, patients with acute type A aortic dissection have a high mortality of 50% within the first 48 hours,[81] therefore, surgery is the treatment of choice. Patients with type B dissection are often treated medically with close surveillance to identify possible progression of the dissection. Herewith, sequential imaging of the thoracic and, if necessary, abdominal aorta is essential. CTA is the imaging technique of choice in patients suspected for aortic dissection in acute setting. CE-MRA is an excellent technique for multiple follow-up examinations, without ionizing radiation or the use of iodinated contrast. For MRI, high sensitivity and specificity of both 98% in the diagnosis of aortic dissection were reported.[82,83]

T1-weighted imaging can determine blood in the aortic wall and additional T2-weighted imaging can further help to analyze the blood compounds characteristics and age of IMH. CE-MRA clearly reveals the extent of aortic dissection and the possible extension into arterial side braches. Moreover, branching arteries originating from the true or false lumen can be evaluated. Both SSFP images and CE-MRA can clearly visualize the intimal flap. However, MIP images may obscure the intimal flap and therefore, dissection may be missed. Therefore, it remains important to review both source images of the CE-MRA sequence, together with SSFP images and MPR in patients with suspicion of or known aortic dissection. It is not advisable to make a diagnosis based solely on the projection images.

Magnetic resonance angiography of the renal arteries

Renal artery stenosis is regarded one of the most common manifestations of systemic atherosclerosis. It is a progressive disease and is more seen in elderly. Increased prevalence in patients with coronary artery disease and peripheral artery disease are reported.[84,85] Typically, stenosis of the renal artery either involves the origin of the renal artery or the proximal third part or it is caused by an aortal atherosclerotic plaque impinging on the ostium of the renal artery. Patients with renal artery stenosis often have bilateral renal artery stenoses.[86] Luminal diameter narrowing of more than 50 to70% is considered hemodynamically significant.

In young patients, renal arterial stenosis can be caused by fibromuscular dysplasia (FMD). FMD is a idiopathic, non-atherosclerotic, segmental disease of the arterial wall leading to stenosis, aneurysm, dissection and/or occlusion of small to medium-sized arteries, especially renal and carotid arteries and predominantly occurs in young and female patients. When the renal arteries are involved, it may cause secondary hypertension.[87]

The standard of reference to determine the diagnosis of renal artery stenosis anatomically is catheter renal angiography, i.e. DSA. Direct measurement of hemodynamic characteristics is possible by involving transstenotic pressure measurements and if necessary, revascularization can be performed immediately. However, DSA has known limitations as the use of ionizing radiation and iodinated contrast. Moreover, DSA is an invasive imaging tool with possible risk of complications.

Nowadays, non-invasive imaging modalities have replaced DSA in the diagnosis and work-up in patients with suspected renal artery stenosis in clinical practice. Doppler ultrasonography is a frequently used imaging modality to evaluate renal vasculature. DUS is a widely available, non-invasive and radiation-free technique that allows anatomic assessment of renal artery stenosis and measurement of renal artery flow patterns. To characterize significant renal artery stenosis, several DUS measures have been proposed, e.g. renal-to-aortic peak systolic ratio,[88,89] and renal peak systolic velocity.[90,91] Zeisbrich et al.[92] showed that real-time contrast-enhanced ultrasonography was superior to conventional Doppler ultrasonography in microvascular perfusion changes in allografts. Contrast-enhanced ultrasonography can play a role as a complementary imaging tool to assess renal artery stenosis and detailed qualitative and quantitative information on renal microvascular perfusion. Doppler ultrasonography is, however, time consuming, highly operator dependent, and can be technical challenging in obese patients.

Modern multi-slice CT scanners permit rapid high resolution imaging with accurate first-pass contrast timing in patients with renal arterial disease. High accuracy of CTA for diagnosing significant atherosclerotic renal stenosis has been reported, with a sensitivity and specificity of 94% and 93%, respectively.[93] Also high sensitivity and specificity of 100% and 99%, respectively was described for detecting in-stent recurrent stenosis in patients following percutaneous revascularization.[94] Limitations of CTA are the use of ionizing radiation and iodinated contrast. Another disadvantage of CTA is its inability to perform physiologic assessment of renal arterial stenosis and, moreover, severe renal artery calcification may obscure arterial lumen narrowing and limiting evaluation of stenosis.

CE-MRA is a reliable and fast non-invasive imaging technique providing accurate visualization of the renal arteries and accessory renal arteries.[95] Meta-analysis showed a sensitivity and specificity of 88% to 100%, respectively.[96] 3D CE-MRA provides anatomic evaluation of renal arteries. Additionally PCA images can be acquired, adding functional information about renal arterial flow (Figure 4.4). In clinical practice, this can help for example in the analysis of the hemodynamic significance of an intermediate-grade renal artery stenosis (40%–70%), which cannot be reliably derived from vessel diameter measurements alone. In these cases, PCA can be used as an adjunct to CE-MRA for assessing and grading the hemodynamic relevance of intermediate-grade renal stenosis for decision on proper treatment strategies.[97,98]

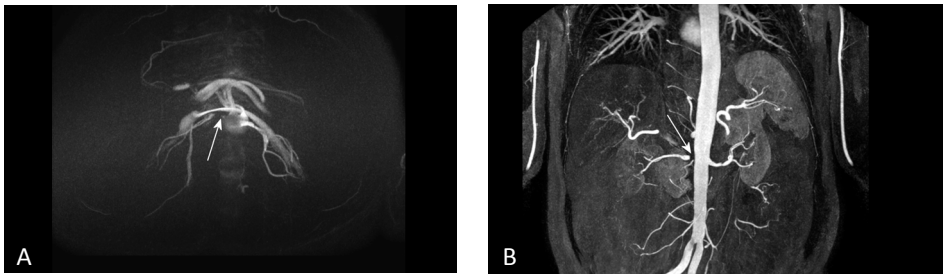

Figure 4.4 **(A)** 3D CE-MRA (maximum-intensity-projection) shows a short stenosis of the right proximal renal artery (arrow). **(B)** 3D phase contrast MRA shows a signal void at the site of the hemodynamic significant stenosis (arrow).

Typically, an MR imaging protocol for renal artery evaluation consists of a survey or localizer sequence, a contrast bolus timing sequence (test bolus or fluoroscopic real-time imaging), a 3D CE-MRA sequence pre- and post-contrast, and a PCA sequence. For optimizing signal and image quality a body phased-array coil should be applied. A fast 2D balanced-gradient-echo sequence or Fast Spin Echo (FSE) sequence can be used as survey sequence. The survey scan is performed in the same breath holding position as utilized for the 3D CE-MRA acquisition. Preferably, this breath holding is end-expiration.[64] A pre-contrast 3D scan is acquired to control proper positioning of the 3D volume and rule out aliasing artifacts. After intravenous administration of Gd contrast (0.1–0.2 mmol/kg body weight), the 3D CE-MRA sequence is performed. Typically, the 3D CE-MRA images have an acquired in-plane resolution of approximately 1 mm × 1 mm and a slice thickness of 2-2.5 mm. The 3D volume is positioned in coronal plane and acquired during breath holding (less than 20 seconds). Following the 3D CE-MRA the PCA sequence is acquired with a standardized typical velocity of 35 cm/s in the right-left direction, 35 cm/s in the anterior-posterior, and 100 cm/s in the feet-head direction, respectively. Post-processing of the acquired 3D CE-MRA and PCA data, using multi-planar reconstruction and maximum intensity projection is essential for renal artery evaluation and permits detailed analysis in all desired planes. In all patients, but especially in those with suspected renal artery stenosis, referred for CE-MRA, the eGFR should be assessed prior to the MRI examination, to rule out possible NFS-related complications.

Significant renal artery stenosis may activate the renin-angiotensin-aldosteron system and is associated with arterial hypertension, ischemic nephropathy, and chronic kidney disease. The main options for treatment of renal arterial stenosis include percutaneous or surgical by-pass revascularization, or medical therapy. Large, randomized trials showed no significant difference in systolic blood pressure[99] or only revealed a reduction of 2 mmHg in systolic blood pressure in patients with

revascularization in combination with medical therapy when compared to medical therapy alone.[100] Moreover, renal artery revascularization did not show significant clinical benefit concerning prevention of clinical events.[99,100]
However, meta-analysis also showed that patients with atherosclerotic renal artery stenosis proofed better control of diastolic blood pressure and a reduction in the mean number of antihypertensive drugs after endovascular treatment.[101,102]
Selected subgroups of patients, e.g. patients with accelerated or malignant hypertension, difficult to control blood pressure, young patients with FMD, or at risk of progressive nephropathy and end-organ failure may benefit from renal arterial revascularization.[103,104]

Magnetic resonance angiography of the mesenteric arteries

Atherosclerotic vascular disease of the mesenteric arteries is the leading cause of chronic mesenteric ischemia (CMI). In asymptomatic elderly patients, significant mesenteric arterial disease, i.e. a stenosis of more than 70% or an occlusion, has been reported in 18% in a population-based prevalence study.[105] However, significant mesenteric arterial stenosis does not necessarily indicate the presence of mesenteric ischemia clinically.[106] The mean reason for this is that the mesenteric arterial circulation contains multiple collateral pathways between the celiac artery, superior mesenteric artery and inferior mesenteric artery. Therefore, involvement of atherosclerosis in the mesenteric arteries in patients with generalized atherosclerosis infrequently leads to symptoms of chronic mesenteric ischemia. The collateral pathways of the mesenteric arterial circulation include the pancreatico-duodenal arcade, arc of Riolan, arc of Buhler, arc of Barkow and the marginal artery of Drummond. In general in patients with symptoms of CMI, two of the three mesenteric arteries show significant stenosis or occlusion.[107,108] Mostly, patients with stenosis of one of the three mesenteric arteries do not present symptoms of CMI,[109] however, CMI has been reported in isolated mesenteric arterial stenosis.[110]
In patients with CMI, mesenteric arterial stenosis or occlusion compromise the blood flow to the intestine leading to postprandial abdominal pain, so-called angine abdominale. Typically, this pain starts within 30 minutes of eating and can last for several hours. This may lead to avoidance of food and significant weight loss. Patients may also present with atypical symptoms as nausea, vomiting, diarrhea, constipation, or colitis. In the majority of patients, diagnosis of CMI is established in an advanced stage of the disease.
The incidence of CMI increases with age, is more prevalent in women and in patients with risk factors for atherosclerotic vascular disease such as history of smoking, hypertension, and hyperlipidemia.[111] Less commonly CMI occurs in young patients

with fibromuscular dysplasia, Takayasu's vasculitis, polyarteritis nodosa, arterial dissection, abdominal aortic anaurysm or post-radiation therapy.

Clinical diagnosis of CMI is established on clinical symptoms and consistent imaging characteristics. Identification of stenotic arterial mesenteric disease without associated clinical symptoms is not diagnostic of CMI.

For diagnosing CMI, conventional DSA remains the reference standard. Advantageously, an endovascular therapeutic procedure can be performed at the time of diagnosis of mesenteric arterial stenosis. However, DSA is an invasive procedure with the already mentioned disadvantages such as the exposure to radiation, nephrotoxic iodinated contrast, and the invasive procedure is associated with complications.[112] In common clinical practice, MRA and CTA have replaced DSA as imaging tool in the work-up of patients suspected for CMI.

In patients suspected of CMI, Doppler ultrasound is useful for screening and is the preferred initial imaging modality. Visualization of high-grade stenoses in the celiac artery or superior mesenteric artery associated with CMI may be technically challenging, especially due to overlying bowel gas or patient's habitus. When compared to angiography, the celiac and superior mesenteric artery are accurately visualized in more than 80% and 90%, respectively.[113] The inferior mesenteric artery can hardly be evaluated by Doppler ultrasound due to its anatomical location.[114] Peak systolic velocity (PSV) has been widely used for evaluating celiac and superior mesenteric arterial disease with a sensitivity and specificity for diagnosing hemodynamically significant stenosis of 92% and 96%, and 87% and 80%, respectively.[115]

Van Petersen et al.[116] showed that stenosis in the celiac or superior mesenteric artery results in an increase of flow velocities in the other mesenteric arteries. The increase in flow was correlated with the presence of collateral vessels. This may lead to overgrading or mimicking stenosis in the other mesenteric artery. Therefore, Doppler ultrasound should be used only as an initial screening imaging tool and in case of demonstrated arterial stenosis further evaluation by performing MRA or CTA is required.

CTA is considered the first-line alternative to diagnostic DSA for evaluation of CMI.[114] Especially in the emergency situation of the suspicion of an acute mesenteric ischemia, CTA is the most appropriate imaging modality. It is a fast non-invasive imaging technique and widely available. Acquired 3D data sets can be post-processed in varying planes and other causes for abdominal pain can be evaluated. For stenosis grading of mesenteric arteries high sensitivity and specificity of 100% and 95%, respectively with DSA as the reference standard were reported.[117] However, diagnostic value of CTA may be limited with the presence of extensive calcifications. Other known drawbacks include the use of radiation and iodinated contrast, therefore, CE-MRA is a an accurate and reliable alternative non-invasive imaging tool for diagnosing CMI. 3D CE-MRA has a high sensitivity and specificity ranging from

92-100% and 95-100%, respectively.[117,118,119] CE-MRA has, however, a limited role in the evaluation of distal mesenteric arteries and depicting stenosis in the inferior mesenteric artery.[120,121]

Routinely, 3D CE-MRA is acquired with the patient in supine position utilizing a surface phased-array coil for optimizing SNR. As with other previously described 3D CE-MRA protocols, the mesenteric arteries are evaluated with a protocol which comprises a survey or localizer sequence, a contrast bolus timing sequence (test bolus or fluoroscopic real-time imaging), and a 3D CE-MRA sequence pre- and post-contrast. Spatial resolution and slice thickness should be tailored for the individual patient that the 3D volume can be imaged in one single breath-hold. The same breath holding position is utilized for the survey scan and the 3D CE-MRA acquisition. The pre-contrast 3D scan can be used to check correct positioning of the 3D volume and rule out aliasing artifacts, as was discussed previously. 3D CE-MRA sequence is performed after intravenous administration of Gd contrast (0.1–0.2 mmol/kg body weight). The 3D volume slab is positioned in sagittal plane, if the primary clinical indication is to determine arterial disease of the mesenteric arteries, which occurs mostly proximal in the course of the mesenteric arteries. Also the coronal plane can be used to include the aorta and portal vein. In addition to the arterial phase, the sequence can be repeated to obtain the portal and systemic venous phase. Typically, images are required with an in-plane resolution of approximately 1–2 mm and a slice thickness of 1–2 mm, resulting in a breath-hold of 10–20 seconds.[122]

CE-MRA should be performed in both inspiration and expiration when median arcuate ligament syndrome is suspected (Figure 4.5). In median arcuate ligament syndrome, the celiac artery is compressed by the central tendon of the diaphragm crura. The classical finding is a smooth narrowing of the proximal celiac artery in expiration, diminishing or disappearing in inspiration. With inspiration, the celiac artery moves inferiorly and more vertically alleviating the compression of the ligamentous band. By performing 3D CE-MRA in both inspiration and expiration the diagnosis can be obtained and differentiated from atherosclerotic arterial disease.

Non-CE- MRA such as TOF and PCA are flow-dependent MR techniques and may suffer from decreased sensitivity and specificity due to slow flow and artefacts from turbulence overestimating stenosis. SSFP techniques demonstrated a superior visualization of the inferior mesenteric artery when compared to CE-MRA[123] and may play a role in patients with contra-indications for intravenous administration of Gd-based or iodinated contrast media.

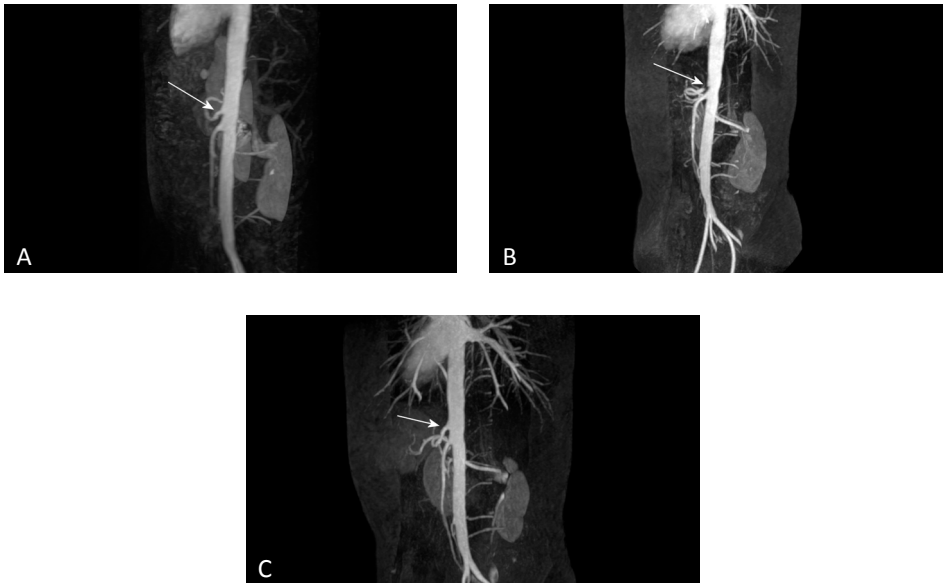

Figure 4.5 A patient diagnosed with the arcuate ligament syndrome shows significant narrowing of the celiac artery (arrow) on CE-MRA (maximum-intensity-projection) during expiration **(A)** disappearing in inspiration **(B)** (arrow). **(C)** shows CE-MRA during inspiration after surgical release of the median arcuate ligament (arrow).

Magnetic resonance angiography of the peripheral arteries

Peripheral arterial disease (PAD) is a common clinical manifestation of atherosclerosis and is – together with coronary artery disease and stroke – one of the leading causes of atherosclerotic cardiovascular morbidity.[124] It has been estimated that around 8.5 million people in the United States of America are effected by PAD over the age of 40 years.[125] Due to raised life expectancy, the prevalence of PAD increased over the last decades by more than 20% and has become a global problem affecting more than 200 million people worldwide,[124] causing a global increase in morbidity and mortality associated with PAD.[126] Prevalence rates increase with age, and the prevalence in men and women is similar.[127] However, in the last decades women experienced a more dramatic increase in morbidity and mortality from PAD when compared with men.[126] Risk factors significantly associated with the incidence of PAD are smoking, diabetes mellitus, hypertension, hypercholesterolemia, and chronic kidney disease.[128] Markers of inflammation and thrombosis are also associated with PAD.[129] Intermittent claudication is the classic symptom in PAD, however described in only about 10% of patients with PAD,[130] whereby men are more likely to have classic symptoms of

claudication. The large majority of patients show a wide range of leg symptoms or are even asymptomatic.

PAD is associated with increased risk for cardiac and cerebral events[131,132] and moreover, several reports showed an up to six times higher risk for mortality from cardiovascular causes and a 2.5 times higher overall mortality rate in patients with symptomatic PAD.[127,133] Therefore, assessment of risk factors for risk stratification in patients with PAD is very relevant.[134]

Assessment of risk factors such as hypertension, diabetes mellitus, body mass index, levels of triglyceride and high-density lipoprotein in blood plasma samples, and ankle-brachial index is essential when risk factor reduction is pursued. Moreover, the usefulness of non-invasive imaging for risk assessment in cardiovascular disease is recognized,[135] e.g. the assessment of MR imaging biomarkers such as mean MRA stenosis and pulse wave velocity showed prognostic value for all-cause mortality and cardiac events in patients with symptomatic PAD.[136]

Clinically, symptoms in patients with PAD can be staged according the Fontaine or Rutherford classification. The Fontaine classification[137,138] is divided in four different stages, stage I: asymptomatic, stage IIa: intermittent claudication after more than 200 meters of pain free walking, stage IIb: intermittent claudication after less than 200 meters of walking, stage III: rest pain or nocturnal pain, and stage IV: ischemic ulcers or gangrene.

The Rutherford classification[137,138] is divided in three grades. Grade I compromises category 0: asymptomatic, category 1: mild claudication, category 2: moderate claudication, and category 3: severe claudication. Grade II compromises category 4: ischemic rest pain, and category 5: minor tissue loss, nonhealing ulcer or focal gangrene. Grade III compromises category 6: major, severe ischemic ulcers or gangrene. Both the Fontaine and the Rutherford classifications may be used routinely in clinical practice or in research settings.

For the evaluation of patients with symptomatic PAD, several non-invasive tests such as segmental blood pressure, pulse volume recording, Doppler ultrasonography and ankle-brachial index (ABI) are widely available. These inexpensive techniques are easily repeatable and commonly used for the initial screening to analyze the presence and location of atherosclerotic arterial disease of the run-off arteries.[139,140] However, Doppler ultrasonography is highly operator dependent[141] and has several other drawbacks, such as hampered evaluation of peripheral arteries in obese patients and it is difficult to obtain consistent high image quality in the run-off vessels distal to the popliteal artery. ABI is commonly used as a first-line diagnostic imaging tool in clinical practice. Normal ABI range of 1.00 to 1.40, and an abnormal value is defined as ≤0.90.[142] ABI values of 0.91 to 0.99 are regarded “borderline” and values >1.40 are an indication for non-compressible arteries. Moreover, several studies reported ABI to predict all-cause mortality and cardiovascular events in cardiovascular disease.[143,144,145] A low ABI is a strong indicator of the presence of PAD, however, due

to false-negative rates a normal ABI does not rule out the risk of PAD[146] and ABI may underestimate the prevalence of atherosclerotic arterial disease of the lower extremities when compared to CE-MRA.[147]

DSA is still considered as a standard reference for the evaluation of stenosis in PAD. However, due to the invasive character and the risk of possible complications DSA is generally not used as a diagnostic imaging tool. Moreover, because of technical developments of non-invasive imaging techniques such as CTA and MRA, DSA is consequently indicated only in patients with symptomatic PAD for whom percutaneous revascularization is planned or in patients with contra-indications for performing a CTA or MRA examination.

For further work-up and planning of revascularization in patients with symptomatic PAD, CTA and MRA are widely available and used in clinical practice. CTA is an accurate technique for evaluating stenosis severity in patients with PAD. Modern multi-slice CT scanners allow rapid acquisition of high-resolution, thin CT images. Accurate timing of the data acquisition during maximal arterial contrast enhancement provides detailed imaging of the run-off arteries. Meta-analysis estimated a sensitivity and specificity for CTA of 96% and 95%, respectively. However, CTA requires radiation and the use of iodinated contrast material as stated before. Moreover, arterial wall calcification may compromise diagnostic image quality and hamper stenosis evaluation especially in patients with diabetes mellitus and renal failure.[148]

For the detection of peripheral arterial disease, CE-MRA is superior to the conventional non-CE-MRA techniques, such as 2D TOF or PCA. These conventional and older non-CE-MRA techniques were highly time consuming and moreover, suffered from artifacts caused by turbulence and in-plane saturation. In a meta-analysis,[149] the sensitivity and specificity for the detection of significant stenosis (>50% luminal reduction) for 2D TOF ranged from 64% to 100% and 68% to 96%, and for CE-MRA 92% to 100% and 91% to 99%, respectively.

In CE-MRA the run-off vessels are imaged during the arterial first pass of gadolinium-based contrast material after intravenous injection (Figure 4.6). Precise bolus timing is essential for CE-MRA. Starting the acquisition too early, when the contrast bolus is still arriving in the vessels of interest, can cause ringing or Maki artefacts.[13] Starting the acquisition too late can cause venous enhancement hampering image quality, especially in de lower legs. Arterial imaging is thus performed in the time window between arterial and venous enhancement. This time window depends on the rate of contrast agent injection, and will be patient specific.[11] Arterial enhancement must coincide with data read-out of the central k-lines, and for improved arterial/venous differentiation, the central k-lines have to be sampled before venous return.

To cover the whole region of the distal abdominal aorta and the run-off vessels, two methods are clinically used: the single-injection 3-station moving-table (bolus-chase) technique and the multi-station/multi-injection method. In both methods, imaging is performed in a coronal orientation with usually three stations with overlapping field-

of-views , covering the complete anatomic region. Typically, the first station covers the distal abdominal aorta and pelvic region, the second station the upper legs and the third station lower legs. The quadrature body coil (QBC) or phased-array surface coils are used for signal transmission and reception. In both techniques, 3D volumes are planned on acquired 2D TOF survey images. Thereafter, pre-contrast mask images are acquired in all stations. Subtraction of the pre-contrast mask images from the contrast-enhanced images will suppress surrounding tissue.[150]

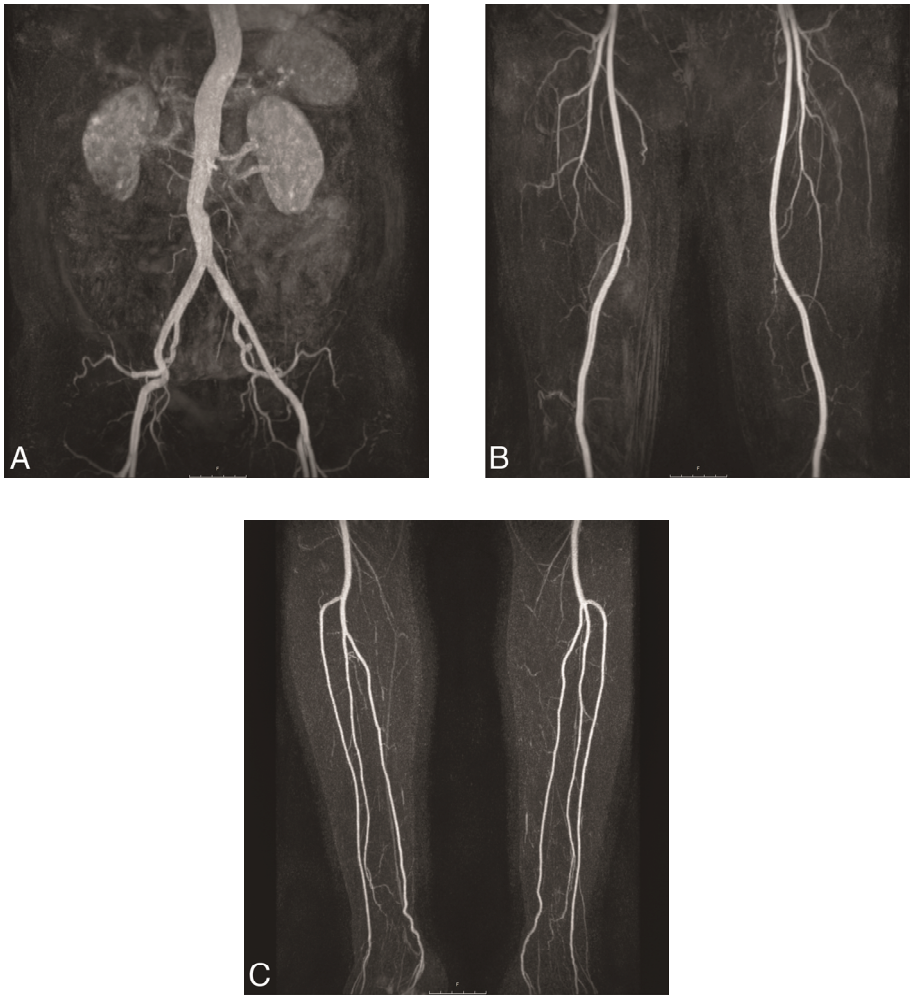

Figure 4.6 CE-MRA showing normal anatomy of the peripheral arteries.

In the bolus-chase technique, a biphasic contrast material injection protocol is typically used. The first half of the contrast bolus is administered at a flow rate of 1.0-1.2 mL/s and the remaining half at 0.5-0.6 mL/s. Contrast injection is followed by a saline flush at 0.5-0.6 mL/s. Modern commercially available 1.5T and 3T MR scanners allow acquisition of CE-MRA of the run-off vessels with a bolus-chase technique with excellent diagnostic performance.[151]

In the multi-station/multi-injection approach, the three regions of the legs stations are acquired sequentially with two or three separate bolus injections of contrast medium.[152] Contrast is injected at a rate of 1 to 1.5 mL/s, resulting in high signal intensity in the arteries. However, a disadvantage of this approach is that it is more time consuming, when compared to the bolus-chase technique. However, in patients with multiple risk factors, adequate arterial enhancement with minimal venous enhancement can be obtained with this technique.[153] The first station covering the distal abdominal aorta and pelvic region is acquired during breath-holding and the acquired resolution is of the first two stations is 1.3 mm × 1.3mm with a slice thickness of 3 mm, typically. The third station covering the lower leg scan be acquired with a submillimeter voxel size, allowing accurate diagnostic evaluation.[154]

Acquired high-resolution image data can be post-processed using multi-planar reconstructions or maximum intensity projections, however for obtaining an adequate diagnosis, evaluation of 2D source images is essential. Furthermore, the role of CE-MRA in the evaluation of possible restenosis in (metallic) stents is limited due to dephasing of MRI signal, causing signal void. New developments in MR imaging technology provide large homogeneous field-of-view at 3T revealing robust CE-MRA of the complete vascular tree of the run-off vessels allowing accurate clinical evaluation of patient on high field 3T scanners.[151] Moreover, two-point Dixon fat suppression allows subtractionless CE- MRA, avoiding possible misregistration artifacts between pre-contrast mask dataset and contrast-enhanced images.[155] Furthermore, new techniques, such as three-station bolus-chase MR angiography with real-time fluoroscopic tracking and precise triggering of table motion can provide high- resolution imaging of the run-off vessels. These new developments potentially can reduce contrast material dose and examination time.[156]

References

1. Prince M, Yucel E, Kaufman J, Harrison D, Geller S. Dynamic gadolinium-enhanced three-dimensional abdominal MR arteriography. J Magn Reson Imaging. 1993;3(6):677-881.
2. Port M, Idée J, Medina C, Robic C, Sabatou M., Corot, C. Efficiency, thermodynamic and kinetic stability of marketed gadolinium chelates and their possible clinical consequences: a critical review. Biometals. 2008;21(4):469-490.
3. Reilly R. Risk for nephrogenic systemic fibrosis with Gadoteridol (ProHance) in patients who are on long-term hemodialysis. Clin J Am Soc Nephrol. 2008;3(3):747-751.
4. Thomson H, Morcos S, Almen T, Bellin M, Bertolotto M, Bongartz G, Clement O, Leander P, Heinz-Peer G, Reimer P, Stacul F, van der Molen A, Webb J. Nephrogenic systemic fibrosis and gadolinium-based contrast media: updated ESUR contrast medium safety committee guidelines. Eur Radiol. 2013;23(2): 307-318.
5. Huckle J, Altun E, Jay M, Semelka R. Gadolinium deposition in humans: when did we learn that gadolinium was deposited in vivo? Invest Radiol. 2016;51(4):236–240.
6. Edwards B, Laumann A, Nardone B, Miller F, Restaino J, Raisch D, McKoy J, Hammel J, Bhatt K, Bauer K, Samaras A, Fisher M, Bull C, Saddleton E, Belknap S, Thomsen H, Kanal E, Cowper S, Abu Alfa A, West D. Advancing pharmacovigilance through academic-legal collaboration: the case of gadolinium-based contrast agents and nephrogenic systemic fibrosis—a Research on Adverse Drug Events and Reports (RADAR) report. Br J Radiol. 2014;87(1042):20140307.
7. Prince M. Gadolinium-enhanced MR aortography. Radiology. 1994;191(1):155-164.
8. Prompona M, Cyran C, Nikolaou K, Bauner K, Reiser M, Huber A. Contrast-enhanced whole-heart MR coronary angiography at 3.0 T using the intravascular contrast agent gadofosveset. Invest Radiol. 2009;44(7):369-374.
9. Jaspers K, Versluis B, Leiner T, Dijkstra P, Oostendorp M, Van Golde J, Post M, Backes W. MR angiography of collateral arteries in a hind limb ischemia model: comparison between blood pool agent Gadomer and small contrast agent Gd-DTPA. PloS One. 2011;6(1):e16159.
10. Wilson G, Hoogeveen R, Willinek W, Muthupillai R, Maki J. Parallel imaging in MR angiography. Top Magn Reson Imaging. 2004;15(3):169-185.
11. Prince M, Chabra S, Watts R, Chen C, Winchester P, Khilnani N, Trost D, Bush H, Kent K, Wang Y. Contrast material travel times in patients undergoing peripheral MR angiography. Radiology. 2002;224(1):55-61.
12. Maki J, Prince M, Chenevert T. Optimizing three-dimensional gadolinium-enhanced magnetic resonance angiography. Invest Radiol. 1998;33(9):528-537.
13. Maki J, Prince M, Londy F, Chenevert T. The effects of time-varying intravascular signal intensity and k-space acquisition order on three-dimensional MR angiography image quality. J Magn Reson Imaging. 1996;6(4): 642-651.
14. Willinek W, Gieseke J, Conrad R, Strunk H, Hoogeveen R, von Falkenhausen M, Keller E, Urbach H, Kuhl C, Schild H. Randomly segmented central k-space ordering in high-spatial-resolution contrast-enhanced MR angiography of the supra-aortic arteries: initial experience. Radiology. 2002; 225(2): 583-588.
15. Grobner T. Gadolinium, a specific trigger for the development of nephrogenic fibrosing dermopathy and nephrogenic systemic fibrosis? Nephrol Dial Transplant. 2006;21(4): 1104-1108.
16. Prince M, Zhang H, Roditi G, Leiner T, Kucharczyk W. Risk factors for NSF: a literature review. J Magn Reson Imaging. 2009;30(6): 1298-1308.
17. Kanda T, Fukusato T, Matsuda M, Toyoda K, Oba H, Kotoku J, Haruyama T, Kitajima K, Furui S. Gadolinium-based contrast agent accumulates in the brain even in subjects without severe renal dysfunction: evaluation of autopsy brain specimens with inductively coupled plasma mass spectroscopy. Radiology. 2015;276(1): 228-232.
18. Kanda T, Ishii K, Kawaguchi H, Kitajima K, Takenaka D. High signal intensity in the dentate nucleus and globus pallidus on unenhanced T1-weighted MR images: relationship with increasing cumulative dose of a gadolinium-based contrast material. Radiology. 2014;270(3): 834-841.

19. Murata N, Gonzalez-Cuyar L, Murata K, Fligner C, Dills R, Hippe D, Maravilla K. Macrocyclic and other non-group 1 gadolinium contrast agents deposit low levels of gadolinium in brain and bone tissue: preliminary results from 9 patients with normal renal function. Invest Radiol. 2016;51(7): 447-453.
20. Wang Y-X, Schroeder J, Siegmund H, Idée J-M, Fretellier N, Jestin-Mayer G, Factor C, Deng M, Kang W, Morcos S. Total gadolinium tissue deposition and skin structural findings following the administration of structurally different gadolinium chelates in healthy and ovariectomized female rats. Quant Imaging Med Surg. 2015;5(4): 534-545.
21. Kanda T, Osawa M, Oba H, Toyoda K, Kotoku J, Haruyama T,Takeshita K, Furui S. High signal intensity in dentate nucleus on unenhanced T1-weighted MR images: association with linear versus macrocyclic gadolinium chelate administration. Radiology. 2015;275(3): 803–809.
22. Radbruch A, Weberling L, Kieslich P, Eidel O, Burth S, Kickingereder P, Heiland S, Wick W, Schlemmer H-P, Bendszus M. Gadolinium retention in the dentate nucleus and globus pallidus is dependent on the class of contrast agent . Radiology. 2015;275(3): 783-791.
23. Simonetti O, Finn J, White R, Laub G, Henry D. “Black blood” T2-weighted inversion-recovery MR imaging of the heart. Radiology. 1996;199(1): 49-57.
24. Miyazaki M, Akahane M. Non-contrast enhanced MR angiography: established techniques. J Magn Reson Imaging. 2012;35(1): 1-19.
25. Miyazaki M, Lee V. Nonenhanced MRangiography. Radiology. 2008;248(1): 20-43.
26. Holloway B, Rosewarne D, Jones R. Imaging of thoracic aortic disease. Br J Radiol. 2011;84(Spec Iss 3): S338-354.
27. Axel L. Blood flow effects in magnetic resonance imaging. Am J Roentgenol. 1984;143(6): 1157-1166.
28. Bradley W, Waluch V. Blood flow: magnetic resonance imaging. Radiology. 1985;154(2): 443-450.
29. Lotz J, Meier C, Leppert A, Galanski M. Cardiovascular flow measurement with phase-contrast MR imaging: basic facts and implementation. Radiographics. 2002;22(3): 651-671.
30. Nelemans P, Leiner T, de Vet H, van Engelshoven J. Peripheral arterial disease: meta-analysis of the diagnostic performance of MR angiography. Radiology. 2000; 217(1): 105-114.
31. Dixon W. Simple proton spectroscopic imaging. Radiology. 1984;153(1): 189-194.
32. Nezafat M, Henningsson M, Ripley D, Dedieu N, Greil G, Greenwood J, Börnert P, Plein S, Botnar R. Coronary MR angiography at 3T: fat suppression versus water-fat separation. J Cardiovasc Magn Reson. 2014;16(Suppl 1): 175.
33. Calkoen E, Roest A, van der Geest R, de Roos A, Westenberg J. Cardiovascular function and flow by 4-dimensional magnetic resonance imaging techniques: new applications. J Thorac Imaging. 2014;29(3): 185-196.
34. Dyverfeldt P, Bissell M, Barker A, Bolger A, Carlhäll C, Ebbers T, Francios C, Frydrychowicz A, Geiger J, Giese D, Hope M, Kilner P, Kozerke S, Myerson S, Neubauer S, Wieben O, Markl M. 4D flow cardiovascular magnetic resonance consensus statement. J Cardiovasc Magn Reson. 2015;17(1): 72.
35. Mitsuzaki K, Yamashita Y, Onomichi M, et al. Delineation of simulated vascular stenosis with Gd-DTPA-enhanced 3D gradient echo MR angiography: An experimental study. J Comput Assist Tomogr. 2000;24(1): 77-82.
36. Korosec F, Mistretta C. MR angiography: basic principles and theory. Magn Reson Imaging Clin N Am. 1998;6(2): 223-256.
37. Inzitari D, Eliasziw M, Gates P, Sharpe B, Chan R, Meldrum H, Barnett H. The causes and risk of stroke in patients with asymptomatic internal-carotid-artery stenosis. N Engl J Med. 2000;342(23): 1693-1701.
38. Mozaffarian D, Benjamin E, Go AS, Arnett D, Blaha M, Cushman M, Das S, de Ferranti S, Després J-P, Fullerton H, Howard V, Huffman M, Isasi C, Jiménez M, Judd S, Kissela B, Lichtman J, Lisabeth L, Liu S, Mackey R, Magid D, McGuire D, Mohler III E, Moy C, Muntner P, Mussolino M, Nasir K, Neumar R, Nichol G, Palaniappan L, Pandey D, Reeves M, Rodriguez C, Rosamond W, Sorlie P, Stein J, Towfighi A, Turan T, Virani S, Woo D, Yeh R, Turner M, on behalf of the American Heart Association Statistics Committee and Stroke Statistics Subcommittee. Heart disease and stroke statistics-2016 update. A report from the American Heart Association. Circulation. 2016; 133(4): 38-361.

39. Amarenco P, Lavallée P, Labreuche J, Albers G, Bornstein N, Canhão P, Caplan L, Donnan G, Ferro J, Hennerici M, Molina C, Rothwell P, Sissani L, Školoudík D, Steg P, Touboul P-J, Uchiyama S, Vicaut E, Wong L. One-year risk of stroke after transient ischemic attack or minor stroke. N Engl J Med. 2016;374(16): 1533-1542.
40. Hankey G, Warlow C, Sellar R. Cerebral angiographic risk in mild cerebrovascular disease. Stroke. 1990;21(2): 209-222.
41. Wardlaw J, Chapel F, Best J, Wartolowska K, Berry E. Noninvasive imaging compared with intra-arterial angiography in the diagnosis of symptomatic carotid stenosis: a meta-analysis. Lancet. 2006;367(9521): 1503-1512.
42. Arous E, Simons J, Flahive J, Beck A, Stone D, Hoel A, Messina L, Schanzer A. National variation in preoperative imaging, carotid duplex ultrasound criteria, and threshold for surgery for asymptomatic carotid artery stenosis. J Vasc Surg. 2015;62(4): 937-944.
43. Brot T, Halperin J, Abbara S, Bacharach J, Barr J, Bush R, Cates C, Creager M, Fowler S, Friday G, Hertzberg V, McIff E, Moore W, Panagos P, Riles Th, Rosenwasser R, Taylor A. 2011 guideline on management of patients with extracranial carotid and vertebral artery disease: executive summary. J Am Coll Cardiol. 2011;57(8): 1002-1044.
44. DeMarco J, Willinek W, Finn J, Huston III J. Current state-of-the-art 1.5T and 3T extracranial carotid contrast-enhanced magnetic resonance angiography. Neuroimag Clin N Am. 2012;22(2): 235-257.
45. Dehkharghani S, Qiu D, Albin L, Saindane A. Dose reduction in contrast-enhanced cervical MR angiography: Field strength dependency of vascular signal intensity, contrast administration, and arteriographic quality. Am J Roentgenol. 2015; 204(6): W701-W706.
46. Tomasian A, Salamon N, Lohan DG, Jalili M, Villablanca J, Finn J. Supraaortic arteries: Contrast material dose reduction at 3.0-T high-spatial-resolution MR angiography-feasibility study. Radiology. 2008;249: 980-990.
47. Townsend T, Saloner D, Pan X, Rapp J. Contrast material-enhanced MRA overestimates severity of carotid stenosis, compared with 3D time-of-flight MRA. J Vasc Surg. 2003;38(1): 36-40.
48. Patel M, Kuntz K, Klufas R, Kim D, Kramer J, Polak J, Skillman J, Whittemore A, Edelman R, Kent K. Preoperative assessment of the carotid bifurcation. Can magnetic resonance angiography and duplex ultrasonography replace contrast arteriography? Stroke. 1995;26(10): 1753-1758.
49. DeMarco J, Schonfeld S, Keller I, Bernstein M. Contrast-enhanced carotid MR angiography with commercially available triggering mechanisms and elliptic centric phase encoding. Am J Roentgenol. 2001;12(3): 175-181.
50. Wright V, Olan W, Dick B, Yu H, Alberts-Grill N, Latour L, Baird A. Assessment of CE-MRA for the rapid detection of supra-aortic vascular disease. Neurology. 2005;65(1): 27-32.
51. Zhao H, Wang J, Liu X, Zhao X, Hippe D, Cao Y, Wan J, Yuan C, Xu J. Assessment of carotid artery atherosclerotic disease by using three-dimensional fast black-blood MR imaging: comparison with DSA. Radiology. 2005;274(2): 508-516.
52. Mihai G, Winner M, Raman S, Rajagopalan S, Simonetti O, Chung Y. Assessment of carotid stenosis using three-dimensional T2-weighted dark blood imaging: initial experience. J Magn Reson Imaging. 2012 Feb;35(2): 449-55.
53. Varennes L, Tahon F, Kastler A, Grand S, Thony F, Baguet J, Detante O, Touzé E, Krainik A. Fibromuscular dysplasia: what the radiologist should know: a pictorial review. Insights Imaging. 2015;6(3): 295-307.
54. Debette S, Leys D. Cervical-artery dissections: predisposing factors, diagnosis, and outcome. Lancet Neurol. 2009; 8(7): 668-678.
55. Ben Hassena W,. Machet A, Edjlali-Goujon M, Legranda L, Ladouxa A, Mellerioa C, Bodiguela E, Gobin-Metteila M-P,Trystrama D, Rodriguez-Regenta C, Masa J-L, Plat M, Oppenheima C, Medera J-F,Naggaraa O. Imaging of cervical artery dissection.Diagn Interv Imaging. 2014; 95(12): 1151-1161.
56. Desjardins B, Dill KE, Flamm SD, Francois CJ, Gerhard-Herman MD, Kalva SP, Mansour MA, Mohler ER 3rd, Oliva IB, Schenker MP, Weiss C, Rybicki FJ; American College of Radiology. ACR Appropriateness Criteria® pulsatile abdominal mass, suspected abdominal aortic aneurysm. Int J Cardiovasc Imaging. 2013;29(1): 177-183.

57. Douglas P, Garcia M, Haines D, Lai W, Manning W, Patel AR, Picard M, Polk D, Ragosta M, Ward R, Weiner R. Appropriate use of echocardiography. J Am Soc Echocardiogr. 2011;24(3): 229-267.
58. Evangelista A, Flachskampf F, Erbel R, Antonini-Canterin F, Vlachopoulos C, Rocchi G, Sicari R, Nihoyannopoulos P, Zamorano J. Echocardiography in aortic diseases: EAE recommendations for clinical practice. Eur J Echocardiogr. 2010;11(3): 645-658.
59. Flachskampf F, Decoodt P, Fraser A, Daniel W, Roelandt J. Recommendations for performing transesophageal echocardiography. Eur J Echocardiogr. 2001;2(1): 8–21.
60. Flachskampf F, Badano L, Daniel W, Feneck R, Fox K, Fraser A, Pasquet A, Pepi M, Perez de Isla L, Zamorano J, Roelandt J, Piérard L. Recommendations for transoesophageal echocardiography-update 2010. Euro Heart J Cardiovasc Imaging. 2010;11(7): 557-576.
61. Sommer T, Fehske W, Holzknecht N, Smekal A, Keller E, Lutterbey G, Kreft B, Kuhl C, Gieseke J, Abu-Ramadan D, Schild H. Aortic dissection: a comparative study of diagnosis with spiral CT, multiplanar transesophageal echocardiography, and MR imaging. Radiology. 1996;199(2): 347-352.
62. Steenburg S, Ravenel J. Acute traumatic thoracic aortic injuries: experience with 64-MDCT. Am J Roentgenol. 2008;191(5): 1564-1569.
63. Erbel R, Aboyans V, Boileau C, Bossone E, Di Bartolomeo R, Eggebrecht H, Evangelista A, Falk V, Frank H, Gaemperli O, Grabenwöger M, Haverich A, Iung B, Manolis A, Meijboom F, Nienaber CA, Roffi M, Rousseau H, Sechtem U, Sirnes P, Allmen R, Vrints C; ESC committee for practice guidelines. 2014 ESC guidelines on the diagnosis and treatment of aortic diseases. Eur Heart J. 2014;35(41): 2873-2926.
64. Plathow C, Ley S, Zaporozhan J, Schöbinger M, Gruenig E, Puderbach M, Eichinger M, Meinzer H, Zuna I, Kauczor H. Assessment of reproducibility and stability of different breath-hold maneuvers by dynamic MRI: comparison between healthy adults and patients with pulmonary hypertension. Eur Radiol. 2006;16(1):173-179.
65. Kramer C, Barkhausen J, Flamm S, Kim R, Nagel E. Standardized cardiovascular magnetic resonance imaging (CMR) protocols, society for cardiovascular magnetic resonance: board of trustees task force on standardized protocols. J Cardiovasc Magn Reson. 2008;10:35.
66. Lim R, Winchester P, Bruno M, Xu J, Storey P, McGorty K, Sodickson D, Srichai M. Highly accelerated single breath-hold noncontrast thoracic MRA: evaluation in a clinical population. Invest Radiol. 2013;48(3): 145-151.
67. Mayil S. Krishnam, Tomasian A, Malik S, Desphande V, Laub G, Ruehm S. Image quality and diagnostic accuracy of unenhanced SSFP MR angiography compared with conventional contrast-enhanced MR angiography for the assessment of thoracic aortic diseases. Eur Radiol. 2010;20(6): 1311–1320.
68. Srichai M, Kim S, Axel L, Babb J, Hecht E. Non-gadolinium-enhanced 3-dimensional magnetic resonance angiography for the evaluation of thoracic aortic disease: a preliminary experience. Tex Heart Inst J. 2010;37(1): 58-65.
69. Hiratzka L, Bakris G, Beckman J, Bersin R, Carr V, Casey D Jr, Eagle K, Hermann L, Isselbacher E, Kazerooni E, Kouchoukos N, Lytle B, Milewicz D, Reich D, Sen S, Shinn J, Svensson L, Williams D; American College of Cardiology Foundation/American Heart Association Task Force on Practice Guidelines; American Association for Thoracic Surgery; American College of Radiology; American Stroke Association; Society of Cardiovascular Anesthesiologists; Society for Cardiovascular Angiography and Interventions; Society of Interventional Radiology; Society of Thoracic Surgeons; Society for Vascular Medicine. 2010 ACCF/AHA/AATS/ACR/ASA/SCA/SCAI/SIR/STS/SVM Guidelines for the diagnosis and management of patients with thoracic aortic disease. A Report of the American College of Cardiology Foundation/American Heart Association Task Force on Practice Guidelines, American Association for Thoracic Surgery, American College of Radiology,American Stroke Association, Society of Cardiovascular Anesthesiologists, Society for Cardiovascular Angiography and Interventions, Society of Interventional Radiology, Society of Thoracic Surgeons,and Society for Vascular Medicine. J Am Coll Cardiol. 2010;55(14): e27-e129.
70. Cozijnsen L, Braam R, Waalewijn R, Schepens M, Loeys B, van Oosterhout M, Barge-Schaapveld D, Mulder B. What is new in dilatation of the ascending aorta? Review of current literature and practical advice for the cardiologist. Circulation. 2011;123(8): 924-928.

71. Svensson L, Adams D, Bonow R, Kouchoukos N, Miller D, O'Gara P, Shahian D, Schaff H, Akins C, Bavaria J, Blackstone E, David T, Desai N, Dewey T, D'Agostino R, Gleason T, Harrington K, Kodali S, Kapadia S, Leon M, Lima B, Lytle B, Mack M, Reardon M, Reece T, Reiss G, Roselli E, Smith C, Thourani V, Tuzcu E, Webb J, Williams M. Aortic valve and ascending aorta guidelines for management and quality measures. Ann Thorac Surg. 2013;95(6 Suppl): S1-66.
72. Mendoza D, Kochar M, Devereux R, Basson C, Min J, Holmes K, Dietz H, Milewicz D, LeMaire S, Pyeritz R, Bavaria J, Maslen C, Song H, Kroner B, Eagle K, Weinsaft J; GenTAC (National registry of genetically triggered thoracic aortic aneurysms and cardiovascular conditions) study investigators. Impact of image analysis methodology on diagnostic and surgical classification of patients with thoracic aortic aneurysms. Ann Thorac Surg. 2011;92(3): 904-912.
73. Landenhed M, Engstrom G, Gottsater A, Caulfield M, Hedblad B, Newton-Cheh C, Melander O, Gustav Smith G. Risk profiles for aortic dissection and ruptured or surgically treated aneurysms: a prospective cohort study. J Am Heart Assoc. 2015 Jan 21;4(1): e001513.
74. Prince M. Gadolinium-enhanced MR aortography. Radiology. 1994;191(1): 155–164.
75. Arlart I, Gerlach A, Kolb M, Erpenbach S, Würstlin S. MR-Angiographie mit Gd-DTPA zum Staging des abdominellen Aortenaneurysmas: Korrelation mit DSA und CT Gadopentate dimeglumine enhanced MR angiography (MRA) for staging AAA: a correlation with DSA and CT. Fortschr Röntgenstr. 1997;167(9): 257-263.
76. Singh K, Bønaa K, Jacobsen B, Bjørk L, Solberg S. Prevalence of and risk factors for abdominal aortic aneurysms in a population-based study: The Tromsø Study. Am J Epidemiol. 2001;154(3): 236-244.
77. Forsdahl S, Singh K, Solberg S, Jacobsen B. Risk factors for abdominal aortic aneurysms: a 7-year prospective study: the Tromsø Study, 1994-2001. Circulation. 2009;119(16): 2202-2208.
78. Tessier D, Stone W, Fow R, Abbas M, Andrews J, Bower T, Gloviczki P. Clinical features and management of splenic artery pseudoaneurysm: case series and cumulative review of literature. J Vasc Surg. 2003;38(5): 969-974.
79. Deipolyi A, Rho J, Khademhosseini A, Oklu R. Diagnosis and management of mycotic aneurysms. Clin Imag. 2016;40(2): 256-262.
80. Christoph A. Nienaber. The role of imaging in acute aortic syndromes. Eur Heart J Cardiovasc Imaging. 2013;14(1): 15-23.
81. Chiappini B, Schepens M, Tan E, Dell' Amore A, Morshuis W, Dossche K, Bergonzini M, Camurri N, Reggiani L, Marinelli G, Di Bartolomeo R. Early and late outcomes of acute type A aortic dissection: analysis of risk factors in 487 consecutive patients. Eur Heart J. 2005;26(2): 180–186.
82. Nienaber C, von Kodolitsch Y, Nicolas V, Siglow V, Piepho A, Brockhoff C, Koschyk D, Spielmann R. The diagnosis of thoracic aortic dissection by noninvasive imaging procedures. N Engl J Med. 1993;328(1): 1–9.
83. Shiga T, Wajima Z, Apfel C, Inoue T, Ohe Y. Diagnostic accuracy of transesophageal echocardiography, helical computed tomography, and magnetic resonance imaging for suspected thoracic aortic dissection systematic review and meta-analysis. Arch Intern Med. 2006;166(13): 1350-1356.
84. Harding M, Smith L, Himmelstein S, Harrison K, Phillips H, Schwab S, Hermiller J, Davidson C, Bashore T. Renal artery stenosis: prevalence and associated risk factors in patients undergoing routine cardiac catheterization. J Am Soc Nephrol. 1992;2(11): 1608-1616.
85. Olin J, Melia M, Young J, Graor R, Risius B. Prevalence of atherosclerotic renal artery stenosis in patients with atherosclerosis elsewhere. Am J Med. 1990;88(1N): 46N-51N.
86. Rimmer J, Gennari F. Atherosclerotic renovascular disease and progressive renal failure. Ann Intern Med. 1993;118(9): 712-719.
87. Sanidas E, Seferou M, Papadopoulos D, Makris A, Viniou N, Chantziara V, Cennimata V, Papademetriou V. Renal fibromuscular dysplasia: a not so common entity of secondary hypertension. J Clin Hypertens. 2016;18(3): 240-246.
88. Kohler T, Zierler R, Martin R, Nicholls S, Bergelin R, Kazmers A, Beach K, Strandness D. Noninvasive diagnosis of renal artery stenosis by ultrasonic duplex scanning. J Vasc Surg. 1986;4(5): 450-456.
89. Taylor D, Kettler M, Moneta G, Kohler T, Kazmers A, Beach K, Strandness D. Duplex ultrasound scanning in the diagnosis of renal artery stenosis: a prospective evaluation. J Vasc Surg. 1988;7(2): 363-369.

90. Olin J, Piedmonte M, Young J, De Anna S, Grubb M, Childs M. The utility of duplex ultrasound scanning of the renal arteries for diagnosing significant renal artery stenosis. Ann Intern Med. 1995;122(1): 833-838.
91. Hoffmann U, Edwards JM, Carter S, Goldman M, Harley J, Zaccardi M, Strandness D. Role of duplex scanning for the detection of atherosclerotic renal artery disease. Kidney Int. 1991;39(6): 1232-1239.
92. Zeisbrich M, Kihm L, Drüschler F, Zeier M, Schwenger V. When is contrast-enhanced sonography preferable over conventional ultrasound combined with Doppler imaging in renal transplantation? Clin Kidney J. 2015;8(5): 606-614.
93. Rountas C, Vlychou M, Vassiou K, Liakopoulos V, Kapsalaki E, Koukoulis G, Fezoulidis I, Stefanidis I. Imaging modalities for renal artery stenosis in suspected renovascular hypertension: prospective intraindividual comparison of color Doppler US, CT angiography, GD-enhanced MR angiography, and digital subtraction angiography. Ren Fail. 2007;29(13): 295-302.
94. Steinwender C, Schutzenberger W, Fellner F, Hönig S, Schmitt B, Focke C, Hofmann R, Leisch F. 64-Detector CT angiography in renal artery stent evaluation: prospective comparison with selective catheter angiography. Radiology. 2009;252(1): 299-305.
95. Bakker J, Beek F, Beutler J, Hene R, de Kort G, de Lange E, Moons K, Mali W. Renal artery stenosis and accessory renal arteries: accuracy of detection and visualization with gadolinium-enhanced breath-hold MR angiography. Radiology. 1998;207(2): 497-504.
96. Vasbinder G, Nelemans P, Kessels A, Kroon A, de Leeuw P, van Engelshoven J. Diagnostic tests for renal artery stenosis in patients suspected of having renovascular hypertension: a meta-analysis. Ann Intern Med. 2001;135(6): 401-411.
97. Prince M, Schoenberg S, Ward J, Londy F, Wakefield T, Stanley J. Hemodynamically significant atherosclerotic renal artery stenosis: MR angiographic features. Radiology. 1997;205(1): 128-136.
98. Leiner T, Nelemans P, de Haan M, de Leeuw P, van Engelshoven J, Vasbinder G. Addition of phase-contrast data to anatomical evaluation substantially improves the diagnostic accuracy of dynamic contrast-enhanced renal MR angiography for the detection of renal artery stenosis. In: RSNA Annual Meeting Abstract Book. 2006:540.
99. ASTRAL Investigators, Wheatley K, Ives N, Gray R, Kalra P, Moss J, Baigent C, Carr S, Chalmers N, Eadington D, Hamilton G, Lipkin G, Nicholson A, Scoble J. Revascularization versus medical therapy for renal-artery stenosis. N Engl J Med. 2009;361(20): 1953-1962.
100. Cooper C, Murphy T, Cutlip D, Jamerson K, Henrich W, Reid D, Cohen D, Matsumoto A, Steffes M, Jaff M, Prince M, Lewis E, Tuttle K, Shapiro J, Rundback J, Massaro J, D'Agostino R, Dworkin L; CORAL Investigators. Stenting and medical therapy for atherosclerotic renal-artery stenosis. N Engl J Med. 2014;370(1): 13-22.
101. Caielli P, Frigo A, Pengo M, Rossito G, Maiolino G, Seccia, T, Calo L, Miotto D, Rossi G. Treatment of atherosclerotic renovascular hypertension: review of observational studies and a meta-analysis of randomized clinical trials. Nephrol Dial Transplant. 2015;30(4): 541-553.
102. Kumbhani D, Bavry A, Harvey J, de Souza R, Scarpioni R, Bhatt D, Kapadia S. Clinical outcomes after percutaneous revascularization versus medical management in patients with significant renal artery stenosis: a meta-analysis of randomized controlled trials. Am Heart J. 2011;161(3): 622-630.
103. Bavishi C, de Leeuw P, Messerli F. Atherosclerotic renal artery stenosis and hypertension: pragmatism, pitfalls, and perspectives Am J Med. 2016;129(6): 635.e5-635.e14.
104. Mohan I, Bourke V. The management of renal artery stenosis: an alternative interpretation of ASTRAL and CORAL. Eur J Vasc Endovasc Surg. 2015;49(4): 465-473.
105. Hansen K, Wilson D, Craven T, Pearce J, English W, Edwards M, Ayerdi J, Burke G. Mesenteric artery disease in the elderly. J Vasc Surg. 2004;40(1): 45-52.
106. Roobottom C, Dubbins P. Significant disease of the celiac and superior mesenteric arteries in asymptomatic patients: predictive value of Doppler sonography. Am J Roentgenol. 1993;161(5): 985–988.
107. Parameshwarappa S, Savlania A, Viswanathan S, Gadhinglajkar S, Raman K, Unnikrishnan M. Chronic mesenteric ischemia and therapeutic paradigm of mesenteric revascularization. Indian J Gastroenterol. 2014;33(2): 169-174.

108. Matsumoto A, Tegtmeyer C, Fitzcharles E, Selby J, Tribble C, Angle J, Kron I. Percutaneous transluminal angioplasty of visceral arterial stenoses: results and long-term clinical follow-up. J Vasc Interv Radiol. 1995;6(2): 165-174.
109. Brandt L, Boley S. AGA technical review on intestinal ischemia. Gastroenterology. 2000;118(5): 954-968.
110. Carrick R, Borge M, Labropolous N, Rodriguez H. Chronic mesenteric ischemia resulting from isolated lesions of the superior mesenteric artery a case report. Angiology. 2005;56(6): 785-788.
111. Cangemi J, Picco M. Intestinal ischemia in the elderly. Gastroenterol Clin North Am. 2009;38(3): 527-540.
112. Balduf L, Langsfeld M, Marek J, Tullis M, Kasirajan K, Matteson B. Complication rates of diagnostic angiography performed by vascular surgeons. Vasc Endovascular Surg. 2002;36(6): 439-445.
113. Moneta G, Lee R, Yeager R, Taylor L, Porter J. Mesenteric duplex scanning: a blinded prospective study. J Vasc Surg. 1993;17(1): 79-84.
114. Oliva I, Davarpanah A, Rybicki F, Desjardins B, Flamm S, Francois C, Gerhard-Herman M, Kalva S, Ashraf Mansour M, Mohler E, Schenker M, Weiss C, Dill K. ACR appropriateness criteria: imaging of mesenteric ischemia. Abdom Imaging. 2013;38(4): 714-719.
115. Moneta GL. Screening for mesenteric vascular insufficiency and follow-up of mesenteric artery bypass procedures. Semin Vasc Surg. 2001;14(3): 186-192.
116. Van Petersen A, Kolkman J, Meerwaldt R, Huisman A, van der Palen J, Zeebregts C, Geelkerken R. Mesenteric stenosis, collaterals, and compensatory blood flow. J Vasc Surg. 2014;60(1): 111–119.
117. Schaefer P, Pfarr J, Trentmann J, Wulff A, Langer C, Siggelkow M, Groß J, Knabe H, Schaefer F. Comparison of noninvasive imaging modalities for stenosis grading in mesenteric arteries. Rofo. 2013;185(7): 628-634.
117. Meaney J, Prince M, Nostrant T, Stanley J. Gadolinium-enhanced MR angiography of visceral arteries in patients with suspected chronic mesenteric ischemia. J Magn Reson Imaging. 1997;7(1): 171–176.
119. Holland G, Dougherty L, Carpenter J, Golden M, Gilfeather M, Slossman F, Schnall M, Axel L. Breath-hold ultrafast three-dimensional gadolinium-enhanced MR angiography of the aorta and the renal and other visceral abdominal arteries. Am J Roentgenol.1996;166(4): 971–81.
120. Jaster A, Choudhery S, Ahn R, Sutphin P, Kalva S, Anderson M, Pillai A. Anatomic and radiologic review of chronic mesenteric ischemia and its treatment. Clin Imaging. 2016;40(5): 961–969.
121. Laissy J, Trillaud H, Douek P. MR angiography: noninvasive vascular imaging of the abdomen. Abdom Imaging. 2002;27(5): 488-506.
122. Hagspiel K, Flors L, Hanley M, Norton P. Computed tomography angiography and magnetic resonance angiography imaging of the mesenteric vasculature. Tech Vasc Interv Radiol. 2015;18(1): 2-13.
123. Iozzelli A, D'Orta G, Aliprandi A, Secchi F, Di Leo G, Sardanelli F. The value of true-FISP sequence added to conventional gadolinium-enhanced MRA of abdominal aorta and its major branches. Eur J Radiol. 2009;72(3): 489-493.
124. Fowkes FG, Rudan D, Rudan I, Aboyans V, Denenberg JO, McDermott MM, Norman PE, Sampson UK, Williams LJ, Mensah GA, Criqui MH. Comparison of global estimates of prevalence and risk factors for peripheral artery disease in 2000 and 2010: a systematic review and analysis. Lancet. 2013;382(9901): 1329–1340.
125. Allison MA, Ho E, Denenberg JO, Langer RD, Newman AB, Fabsitz RR, Criqui MH. Ethnic-specific prevalence of peripheral arterial disease in the United States. Am J Prev Med. 2007;32(4): 328–333.
126. Sampson UK, Fowkes FG, McDermott MM, Criqui MH, Aboyans V, Norman PE, Forouzanfar MH, Naghavi M, Song Y, Harrell FE Jr, Denenberg JO, Mensah GA, Ezzati M, Murray C. Global and regional burden of death and disability from peripheral artery disease: 21 world regions, 1990 to 2010. Glob Heart. 2014;9(1): 145-158.
127. Norgren L, Hiatt WR, Dormandy JA, Nehler MR, Harris KA, Fowkes FG; TASC II Working Group. Inter-society consensus for the management of peripheral arterial disease (TASC II). J Vasc Surg. 2007;45(suppl S): S5-S67.
128. Eraso LH, Fukaya E, Mohler ER 3rd, Xie D, Sha D, Berger JS. Peripheral arterial disease, prevalence and cumulative risk factor profile analysis. Eur J Prev Cardiol. 2014;21(6): 704-711.
129. Khawaja FJ, Kullo IJ. Novel markers of peripheral arterial disease. Vasc Med. 2009; 4(4): 381-392.

130. Hirsch AT, Criqui MH, Treat-Jacobson D, Regensteiner JG, Creager MA, Olin JW, Krook SH, Hunninghake DB, Comerota AJ, Walsh ME, McDermott MM, Hiatt WR. Peripheral arterial disease detection, awareness, and treatment in primary care. JAMA. 2001;286(11): 1317–1324.
131. Criqui MH, Ninomiya JK, Wingard DL, Ji M, Fronek A. Progression of peripheral arterial disease predicts cardiovascular disease morbidity and mortality. J Am Coll Cardiol. 2008; 52(21): 1736-1742.
132. Araki Y, Kumakura H, Kanai H, Kasama S, Sumino H, Ichikawa A, Ito T, Iwasaki T, Takayama Y, Ichikawa S, Fujita K, Nakashima K, Minami K, Kurabayashi M. Prevalence and risk factors for cerebral infarction and carotid artery stenosis in peripheral arterial disease. Atherosclerosis 2012;223(2): 473-477.
133. Sigvant B, Lundin F, Wahlberg E. The risk of disease progression in peripheral arterial disease is higher than expected: a meta-analysis of mortality and disease progression in peripheral arterial disease. Eur J Vasc Endovasc Surg. 2016;51(3): 395-403.
134. Goff DC Jr, Lloyd-Jones DM, Bennett G, Coady S, D'Agostino RB Sr, Gibbons R, Greenland P, Lackland DT, Levy D, O'Donnell CJ, Robinson JG, Schwartz JS, Shero ST, Smith SC Jr, Sorlie P, Stone NJ, Wilson PW; American College of Cardiology/American Heart Association Task Force on Practice Guidelines 2013 ACC/AHA guideline on the assessment of cardiovascular risk: a report of the American College of Cardiology/American Heart Association Task Force on Practice Guidelines. J Am Coll Cardiol. 2014;63(25): 2935-2959.
135. Greenland P, Alpert JS, Beller GA, Benjamin EJ, Budoff MJ, Fayad ZA, Foster E, Hlatky MA, Hodgson JM, Kushner FG, Lauer MS, Shaw LJ, Smith SC Jr, Taylor AJ, Weintraub WS, Wenger NK, Jacobs AK, Smith SC Jr, Anderson JL, Albert N, Buller CE, Creager MA, Ettinger SM, Guyton RA, Halperin JL, Hochman JS, Kushner FG, Nishimura R, Ohman EM, Page RL, Stevenson WG, Tarkington LG, Yancy CW; American College of Cardiology Foundation; American Heart Association. ACCF/AHA guideline for assessment of cardiovascular risk in asymptomatic adults: a report of the American College of Cardiology Foundation/American Heart Association Task Force on Practice Guidelines. J Am Coll Cardiol. 2010;56(25): e50-e103.
136. Van den Bosch H, Westenberg J, Setz-Pels W, Kersten E, Tielbeek A, Duijm L, Post J, Teijink J, de Roos A. Prognostic value of cardiovascular MR imaging biomarkers on outcome in peripheral arterial disease: a 6-year follow-up pilot study. Int J Cardiovasc Imaging. (Epub ahead of print).
137. Dormandy JA, Rutherford RB. Management of peripheral arterial disease (PAD). TASC Working Group. TransAtlantic Inter-Society Consensus (TASC) J Vasc Surg. 2000 Jan;31(1): S1–S296.
138. Norgren L, Hiatt WR, Dormandy JA, Nehler MR, Harris KA, Fowkes FG; TASC II Working Group. Inter-Society Consensus for the Management of Peripheral Arterial Disease (TASC II). J Vasc Surg. 2007 Jan;45(Suppl S): S5-67.
139. Hirsch AT, Haskal ZJ, Hertzer NR, Bakal CW, Creager MA, Halperin JL, Hiratzka LF, Murphy WR, Olin JW, Puschett JB, Rosenfield KA, Sacks D, Stanley JC, Taylor LM Jr, White CJ, White J, White RA, Antman EM, Smith SC Jr, Adams CD, Anderson JL, Faxon DP, Fuster V, Gibbons RJ, Hunt SA, Jacobs AK, Nishimura R, Ornato JP, Page RL, Riegel B; American Association for Vascular Surgery; Society for Vascular Surgery; Society for Cardiovascular Angiography and Interventions; Society for Vascular Medicine and Biology; Society of Interventional Radiology; ACC/AHA Task Force on Practice Guidelines Writing Committee to Develop Guidelines for the Management of Patients With Peripheral Arterial Disease; American Association of Cardiovascular and Pulmonary Rehabilitation; National Heart, Lung, and Blood Institute; Society for Vascular Nursing; TransAtlantic Inter-Society Consensus; Vascular Disease Foundation. ACC/AHA 2005 Practice guidelines for the management of patients with peripheral arterial disease (lower extremity, renal, mesenteric, and abdominal aortic): a collaborative report from the American Association for Vascular Surgery/Society for Vascular Surgery, Society for Cardiovascular Angiography and Interventions, Society for Vascular Medicine and Biology, Society of Interventional Radiology, and the ACC/AHA Task Force on Practice Guidelines (Writing Committee to Develop Guidelines for the Management of Patients With Peripheral Arterial Disease): endorsed by the American Association of Cardiovascular and Pulmonary Rehabilitation; National Heart, Lung, and Blood Institute; Society for Vascular Nursing; TransAtlantic Inter-Society Consensus; and Vascular Disease Foundation. Circulation. 2006;113(11): e463-654.

140. Rooke TW, Hirsch AT, Misra S, Sidawy AN, Beckman JA, Findeiss LK, Golzarian J, Gornik HL, Halperin JL, Jaff MR, Moneta GL, Olin JW, Stanley JC, White CJ, White JV, Zierler RE; Society for Cardiovascular Angiography and Interventions; Society of Interventional Radiology; Society for Vascular Medicine; Society for Vascular Surgery. 2011 ACCF/AHA focused update of the guideline for the management of patients with peripheral artery disease (updating the 2005 guideline): a report of the American College of Cardiology Foundation/ American Heart Association Task Force on Practice Guidelines. J Am Coll Cardiol. 2011;58(19): 2020-2045.
141. O'Keeffe ST, Persson AV. Use of noninvasive vascular laboratory in diagnosis of venous and arterial disease. Cardiol Clin. 1991;9(3):429–442.
142. Ankle Brachial Index Collaboration, Fowkes FG, Murray GD, Butcher I, Heald CL, Lee RJ, Chambless LE, Folsom AR, Hirsch AT, Dramaix M, deBacker G, Wautrecht JC, Kornitzer M, Newman AB, Cushman M, Sutton-Tyrrell K, Fowkes FG, Lee AJ, Price JF, d'Agostino RB, Murabito JM, Norman PE, Jamrozik K, Curb JD, Masaki KH, Rodríguez BL, Dekker JM, Bouter LM, Heine RJ, Nijpels G, Stehouwer CD, Ferrucci L, McDermott MM, Stoffers HE, Hooi JD, Knottnerus JA, Ogren M, Hedblad B, Witteman JC, Breteler MM, Hunink MG, Hofman A, Criqui MH, Langer RD, Fronek A, Hiatt WR, Hamman R, Resnick HE, Guralnik J, McDermott MM. Ankle brachial index combined with Framingham Risk Score to predict cardiovascular events and mortality: a meta-analysis. JAMA. 2008;300(2): 197-208.
143. Newman AB, Shemanski L, Manolio TA, Cushman M, Mittelmark M, Polak JF, Powe NR, Siscovick D. Ankle-arm index as a predictor of cardiovascular disease and mortality in the Cardiovascular Health Study: the Cardiovascular Health Study Group. Arterioscler Thromb Vasc Biol.1999;19(3): 538-545.
144. McDermott MM, Feinglass J, Slavensky R, Pearce WH. The ankle-brachial index as a predictor of survival in patients with peripheral vascular disease. J Gen Intern Med. 1994;9(8): 445-449.
145. McKenna M, Wolfson S, Kuller L. The ratio of ankle and arm arterial pressure as an independent predictor of mortality. Atherosclerosis. 1991;87(2-3): 119-128.
146. Doobay AV, Anand SS. Sensitivity and specificity of the ankle-brachial index to predict future cardiovascular outcomes: a systematic review. Arterioscler Thromb Vasc Biol. 2005;25(7): 1463–1469.
147. Wikström J, Hansen T, Johansson L, Lind L, Ahlström H. Ankle brachial index <0.9 underestimates the prevalence of peripheral artery occlusive disease assessed with whole-body magnetic resonance angiography in the elderly. Acta Radiol. 2008;49(2):143-149.
148. Meyer BC, Werncke T, Foert E, Kruschewski M, Hopfenmüller W, Ribbe C, Wolf KJ, Albrecht T. Do the cardiovascular risk profile and the degree of arterial wall calcification influence the performance of MDCT angiography of lower extremity arteries? Eur Radiol. 2010;20(2):497-505.
149. Nelemans PJ, Leiner T, de Vet HC, van Engelshoven JM. Peripheral arterial disease: meta-analysis of the diagnostic performance of MR angiography. Radiology. 2000;217(1): 105-114.
150. Ho KY, de Haan MW, Kessels AG, Kitslaar PJ, van Engelshoven JM. Peripheral vascular tree stenosis: detection with subtracted and nonsubtracted MR angiography. Radiology. 1998;206(3): 673-681.
151. van den Bosch HC, Westenberg JJ, Caris R, Duijm LE, Tielbeek AV, Cuypers PW, de Roos A. Peripheral arterial occlusive disease: 3.0-T versus 1.5-T MR angiography compared with digital subtraction angiography. Radiology. 2013;266(1): 337-346.
152. Watanabe Y, Dohke M, Okumura A, Amoh Y, Ishimori T, Oda K, Hayashi T, Hiyama A, Dodo Y. Dynamic subtraction contrast-enhanced MR angiography: Technique, clinical applications, and pitfalls. Radiographics. 2000;20(1): 135-152.
153. Dinter DJ, Neff KW, Visciani G, Lachmann R, Weiss C, Schoenberg SO, Michaely HJ. Peripheral bolus-chase MR angiography: analysis of risk factors for nondiagnostic image quality of the calf vessels- a combined retrospective and prospective study. Am J Roentgenol. 2009;193(1): 234-240.
154. Bezooijen R, van den Bosch HC, Tielbeek AV, Thelissen GR, Visser K, Hunink MG, Duijm LE, Wondergem J, Buth J, Cuypers PW. Peripheral arterial disease: sensitivity-encoded multiposition MR angiography compared with intraarterial angiography and conventional multiposition MR angiography. Radiology. 2004;231(1): 263-271.
155. Leiner T, Habets J, Versluis B, Geerts L, Alberts E, Blanken N, Hendrikse J, Vonken EJ, Eggers H. Subtractionless first-pass single contrast medium dose peripheral MR angiography using two-point Dixon fat suppression. Eur Radiol. 2013;23(8): 2228-2235.

156. Johnson CP, Weavers PT, Borisch EA, Grimm RC, Hulshizer TC, LaPlante CC, Rossman PJ, Glockner JF, Young PM, Riederer SJ. Three-station three-dimensional bolus-chase MR angiography with real-time fluoroscopic tracking. Radiology. 2014;272(1): 241-251.